Potent, Small-Molecule Inhibitors of Human Mast Cell Tryptase. Antiasthmatic Action of a Dipeptide-Based Transition-State Analogue Containing a Benzothiazole Ketone

Michael J. Costanzo,[†] Stephen C. Yabut,[†] Harold R. Almond, Jr.,[†] Patricia Andrade-Gordon,[†] Thomas W. Corcoran,[†] Lawrence de Garavilla,[†] Jack A. Kauffman,[†] William M. Abraham,[‡] Rosario Recacha,[§] Debashish Chattopadhyay,[§] and Bruce E. Maryanoff*[,†]

Drug Discovery, Johnson & Johnson Pharmaceutical Research & Development, Spring House, Pennsylvania 19477-0776, Division of Pulmonary Disease, University of Miami at Mount Sinai Medical Center, Miami Beach, Florida 33140, and Centre for Macromolecular Studies, University of Alabama at Birmingham, Birmingham, Alabama 35294

Received January 30, 2003

Inhibitors of human mast cell tryptase (EC 3.4.21.59) have therapeutic potential for treating allergic or inflammatory disorders. We have investigated transition-state mimetics possessing a heterocycle-activated ketone group and identified in particular benzothiazole ketone (2*S*)-**6** (RWJ-56423) as a potent, reversible, low-molecular-weight tryptase inhibitor with a K_i value of 10 nM. A single-crystal X-ray analysis of the sulfate salt of (2*S*)-**6** confirmed the stereochemistry. Analogues **12** and **15**−**17** are also potent tryptase inhibitors. Although RWJ-56423 potently inhibits trypsin (K_i = 8.1 nM), it is selective vs other serine proteases, such as kallikrein, plasmin, and thrombin. We obtained an X-ray structure of (2*S*)-**6** complexed with bovine trypsin (1.9-Å resolution), which depicts inter alia a hemiketal involving Ser-189, and hydrogen bonds with His-57 and Gln-192. Aerosol administration of **6** (2*R*,2*S*; RWJ-58643) to allergic sheep effectively antagonized antigen-induced asthmatic responses, with 70−75% blockade of the early response and complete ablation of the late response and airway hyperresponsiveness.

Activated mast cells secrete numerous proinflammatory mediators including histamine, arachidonate metabolites, and proteases. An important mediator is the serine protease tryptase (EC 3.4.21.59), which is a heparin-associated, homotetrameric trypsin-like enzyme that constitutes 20−25% of the total protein of human mast cells.[1−3] Since tryptase is stored in a catalytically active form (rather than as a zymogen) within the secretory granules and released on stimulation, this enzyme is thought to be highly relevant to mast cell-dependent inflammatory conditions.[1−3] Indeed, tryptase has been directly implicated in the pathology of asthma.[4] Consequently, inhibitors of human mast cell tryptase have therapeutic potential for treating allergic or inflammatory disorders such as asthma, vascular injury (e.g., restenosis and atherosclerosis), inflammatory bowel disease, and psoriasis.[5] In this respect, tryptase inhibitors have attracted therapeutic interest, and several types of compounds have been reported,[5,6] such as APC-366 (**1**), which advanced into phase 2 clinical trials but was discontinued,[5a,b] Babim (**2**),[6a] and bifunctional ligand **3** (Chart 1).[6b]

The biological mechanisms by which tryptase contributes to cellular inflammatory responses are not yet completely understood. Although tryptase cleaves and inactivates certain proteins, its range of activity is somewhat limited. On the other hand, tryptase can be particularly detrimental because there are no endogenous protease inhibitors for it. Interestingly, tryptase is one of the few proteases (trypsin being the other) that can effectively activate protease-activated receptor-2 (PAR-2), a tethered-ligand G-protein-coupled receptor, by cleavage of its elongated, extracellular N-terminus.[7] PAR-2, which has been implicated in various inflammatory processes, may be responsible for some of the physiological and pathophysiological effects of tryptase. Since no receptor antagonists for PAR-2 have yet been identified, inhibitors of tryptase offer one of the few means for interrupting PAR-2 activity.

Our interest in tryptase emerged from the confluence of research on thrombin inhibitors[8] and PAR-2.[9] In studying tripeptide heterocycle-activated ketones that potently inhibit thrombin, such as RWJ-50353 (**4**; K_i = 0.19 nM),[8a,b] we probed the minimally acceptable pharmacophore by eliminating different segments of the molecule. We prepared **5** (RWJ-51084), which is only comprised of a single amino acid residue and found it to be a weak thrombin inhibitor (K_i = 12 300 nM), but a reasonably potent inhibitor of trypsin (K_i = 30 nM).[10] Subsequently, we learned that **5** also effectively inhibits tryptase, with a K_i value of 88 nM (Table 1), while being quite selective over other serine proteases such as kallikrein, factor Xa, and chymotrypsin. This level of inhibitory potency is rather impressive given the relatively low molecular weight (MW = 387.5) and simple structure of **5**. Our reported X-ray structure determination on a cocrystal of **5** (actually the 2*S* enantiomer) with trypsin[10] shows the inhibitor occupying the active site with its guanidine group in the S1 specificity pocket

* Address correspondence to this author. E-mail: bmaryano@prdus.jnj.com. Fax: 215-628-4985.
[†] Johnson & Johnson Pharmaceutical Research & Development (formerly The R. W. Johnson Pharmaceutical Research Institute).
[‡] University of Miami at Mount Sinai Medical Center.
[§] University of Alabama at Birmingham.

10.1021/jm030050p CCC: $25.00
Published on Web 08/05/2003

Table 1. Chemical Properties and Enzyme Inhibition Data[a]

compd	salt	2*S*/2*R*[b]	tryptase K_i, nM[c]	trypsin K_i, nM[c]
4	TFA	49:1	6.5 ± 3.0 (3)	3.1 ± 1.7 (3)[d]
5	TFA	1.7:1[e]	88 ± 13 (4)	30 ± 6 (6)
(2*S*)-**6**	HNO_3	32:1	10 ± 3 (7)[f]	8.1 ± 1.8 (4)[f]
(2*R*)-**6**	HNO_3	1:39	380 ± 120 (6)	170 ± 100 (6)
6	HCl	1.2:1	22 ± 5 (13)	6.0 ± 1.0 (9)
12	TFA	1.0:1[g]	19 ± 7 (8)	4.0 ± 1.0 (4)
13	TFA	1:2.5[g]	14 000 ± 600 (2)[h]	960 ± 250 (4)[h]
14	TFA	8.4:1	73 ± 22 (8)	9.9 ± 1.3 (3)
15	TFA	1.5:1	38 ± 14 (5)	9.1 ± 3.8 (3)
16	TFA	2.5:1[i]	20 ± 5 (5)	53 ± 28 (5)[h]
17	TFA	1.2:1	41 ± 14 (6)	7 (1)
18	TFA	ND	470 ± 90 (3)	260 ± 110 (2)[h]
19	TFA	2.1:1	33 ± 9 (3)	38 (1)[h]
20	TFA	2.8:1[g]	250 ± 120 (5)	160 ± 90 (8)[h]
21	TFA	2.5:1[g]	180 ± 60 (3)	81 ± 40 (3)
22	TFA	1.1:1	90 ± 25 (7)	16 ± 3 (3)
23	TFA	–[j]	NA (2)	NA (2)
24	TFA	ND	NA (1)	NA (1)
25	TFA	–	NA (3)	NA (2)
2[k]	HCl	–	140 ± 20 (16)	100 ± 15 (3)

[a] All compounds were isolated and purified by reverse-phase HPLC (typically water/MeCN/CF_3CO_2H, 70:30:0.1) and lyophilized as trifluoroacetate (TFA) hydrates, except where noted. All compounds were characterized by 300-MHz ^{1}H NMR and electrospray MS; also, they were judged to be at least 95% pure by analytical HPLC. The compounds are represented by standard molecular formulas with the following adducts: **2** (3.0 HCl, 4.3 water), **4** (2.3 TFA, 0.8 water), **5** (1.25 TFA, 0.75 water), (2*S*)-**6** (1.0 HNO_3), (2*R*)-**6** (1.0 HNO_3, 0.3 TFA, 1.4 water), **6** (2.5 HCl, 2.2 water), **12** (1.3 TFA, 1.4 water), **13** (1.1 TFA, 1.1 water), **14** (1.2 TFA, 1.0 water), **15** (1.2 TFA, 0.8 water), **16** (1.2 TFA, 1.0 water), **17** (1.2 TFA, 0.5 water), **18** (1.28 TFA, 0.3 water), **19** (1.25 TFA, 1.15 water), **20** (1.3 TFA, 0.75 water), **21** (1.2 TFA, 1.0 water), **22** (1.0 TFA, 1.6 water), **23** (1.2 TFA, 1.0 water), **24** (1.0 water), **25** (1.2 TFA, 1.0 water). Microanalytical data (C, H, N; and water) were within the accepted range, unless noted otherwise. Information on the composition, microanalytical data, and enzymatic assays is given in the Supporting Information. The composition of **12**, **14**, **16**, **18**, **21**, and **23**–**25** was presumed to be 1.2 TFA and 1.0 water for biological testing purposes because there was an insufficient quantity of material to conduct combustion microanalysis. [b] The 2*S*/2*R* epimeric ratio was determined by analytical HPLC, except where otherwise noted. ND = not determined. [c] K_i values except where noted otherwise. NA = not active (<10% inhibition at 100 μM). The number of experiments (N) is indicated in parentheses; standard errors are given for $N > 1$. [d] Value taken from ref 8a. [e] Determined by ^{13}C NMR via the integrals for the peaks at 122.32 and 122.16 ppm, respectively, in the presence of 4.3 equiv of (*R*)-(−)-2,2,2-trifluoro-1-(9-anthryl)ethanol in $CDCl_3$ at 40 °C. [f] IC_{50} values: tryptase, 29 ± 12 (N = 5); trypsin, 22 ± 12 (N = 5). [g] Determined by ^{1}H NMR via the ratio of 2*S* and 2*R* methine proton integrations. [h] IC_{50} value. [i] Determined by ^{1}H NMR via the ratio of methyl proton integrations. [j] Mixture of four unassigned stereoisomers; ratio of 5:4.7:3:1 as determined by ^{1}H NMR via the *H*C−OH methine proton integrations. [k] Reference tryptase inhibitor.

complexed to Asp-189, its ketone involved in a hemiketal bond with the Oγ of Ser-195, and its benzothiazole nitrogen hydrogen bonded to Nϵ of His-57.[8a,11] A comparison of this structural information with the active site of human β-tryptase,[3] by using computer graphics, revealed an opportunity to manipulate **5** to enhance potency as a tryptase inhibitor. In this manner, we discovered the potent, reversible, low-molecular-weight tryptase inhibitor RWJ-56423, (2*S*)-**6**. Herein, we present the tryptase inhibitory activity for (2*S*)-**6** and various analogues, an X-ray crystal structure of (2*S*)-**6** complexed with bovine trypsin, and in vivo bioactivity for **6** (2*R*,2*S* mixture; RWJ-58643) in allergen-sensitized sheep.[12]

Results and Discussion

Drug Design. To explore structure vs activity surrounding **5**, and to enhance potency and selectivity, we considered introducing some additional sites for interaction with groups in the active site of tryptase, particularly around the S2 region. Since thrombin inhibitor **4** is also a potent inhibitor of tryptase, with a single-digit nanomolar K_i value (Table 1), we considered converting the cyclopentyl ring of **5** into an L-proline and attaching simple *N*-acyl groups. An *N*-acyl-L-proline could introduce a hydrogen bond between the acyl carbonyl and the backbone NH of Gly-216 in the active-site β-sheet.[3] Secondarily, we thought that a polar group, such as a hydroxyl, on the proline ring might provide an additional hydrogen bond with the Gln-98 amide side chain of tryptase. Compounds with these and related modifications were synthesized and bioassayed, thereby achieving a potency improvement of approximately 10-fold with the best analogues, such as (2*S*)-**6**.

Synthetic Chemistry. Representative chemistry is given for target compound (2*S*)-**6**, which was synthesized according to the route outlined in Scheme 1. Commercially available methyl 4-benzyloxy-L-prolinate, **7**, was converted by *N*-acetylation and ester saponification to **8**[13] in 41% yield. Arginine Weinreb amide **9**[14] was reacted with excess 2-lithiobenzothiazole at low temperature, and the intermediate ketone was purified by chromatography on silica gel (EtOAc/hexane, 3:2) and then reduced with $NaBH_4$ to a diastereomeric mixture of alcohols (ca. 1:1), which was deprotected to give **10**. The amino group was acylated with **8** to furnish **11**, which was purified by chromatography on silica gel (CH_2Cl_2/MeOH, 19:1), and the alcohol was oxidized with the Dess−Martin periodinane to the ketone, which was largely comprised of the L-arginine isomer.[15] Treatment with anhydrous HF removed both the *p*-tosyl and benzyl moieties, and the resultant (2*S*)-**6** was purified by reverse-phase HPLC (water/MeCN/CF_3CO_2H, 90:10:0.2 to 70:30:0.2; Bondapak C-18) and then converted into an HCl salt. Most of the other analogues discussed herein, **12**–**20** (Chart 2; Table 1), were prepared in a similar fashion. The syntheses of **6** and **8**–**25** are described in the Experimental Section.

As noted above,[15] (2*S*)-**6** can easily suffer base-induced epimerization because of its labile proton α to the keto group. Stability studies on closely related **4** in rat and rabbit plasma showed that the arginine α-proton is completely equilibrated in 2 h under physiological conditions (pH 7.4, 37 °C). Consequently, we also prepared a mixture of epimers, **6**, by equilibrating (2*S*)-**6** prior to HPLC purification and HCl salt formation (1.2:1 ratio of epimers). This epimeric mixture was used for antiasthma studies in conscious allergic sheep.[16]

Enzyme Inhibition. Our compounds, along with reference inhibitor **2**, were tested for inhibition of human β-tryptase and bovine trypsin (Table 1). The data illustrate the importance of the native 2*S* absolute stereochemistry in both the arginine and proline moieties for high affinity: cf. (2*S*)-**6** with (2*R*)-**6**; **12** with **13**. As expected, a basic side chain substituent is essential for potent inhibition: cf. **24** with **6** and **22**. Although an activated ketone is required for strong inhibition, contributions from P2 are equally important: cf. **6** with **23** and **25**. In addition, hydrophobic

Chart 1

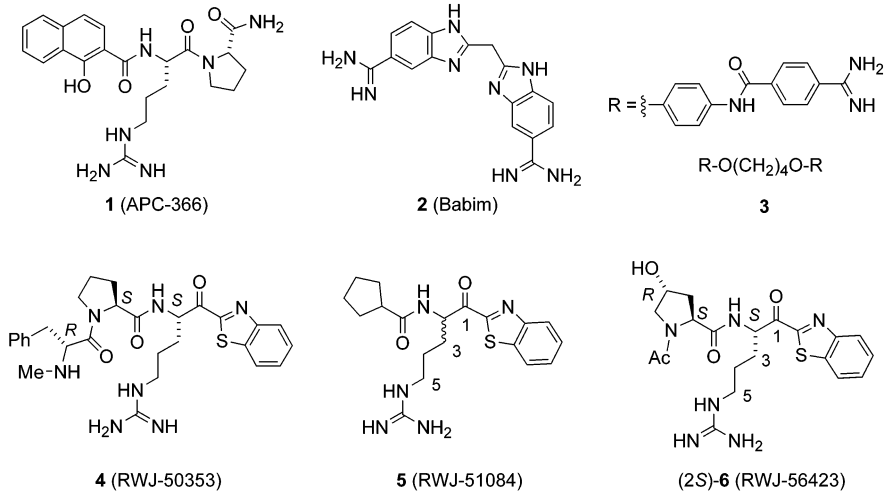

Scheme 1. Synthesis of (2*S*)-**6**

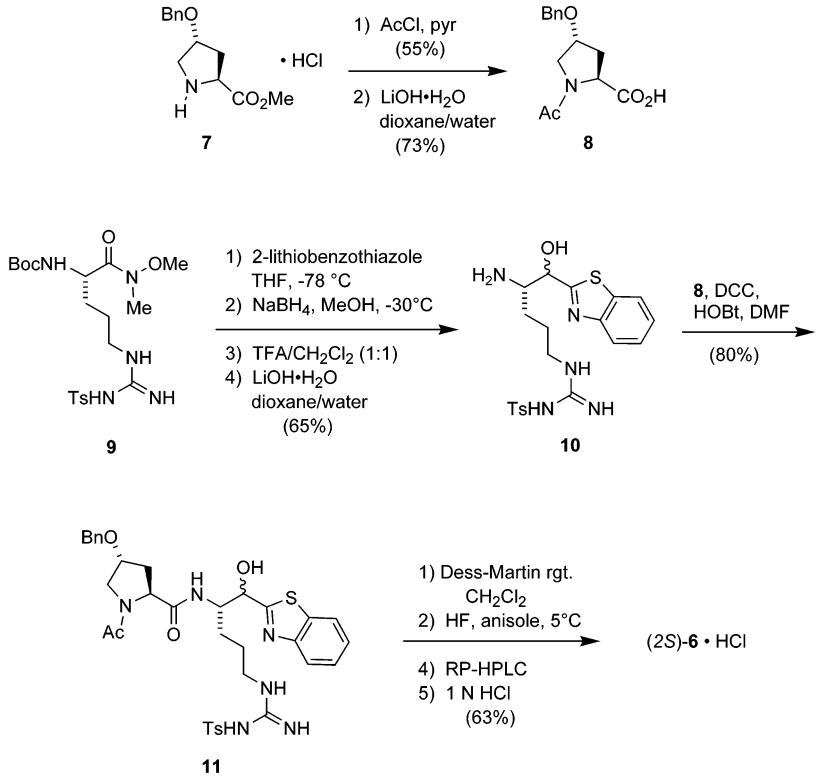

interactions of the P2 substituent are critical for good affinity: cf. **17** with **18**. A benzothiazole group provided a more potent inhibitor than a thiazole group by a factor of ca. 8: cf. **6** with **21**. Acetyl substitution on proline (**12**) led to affinity increases of 1.7-fold relative to mesyl (**19**) and 13-fold relative to benzoyl (**20**). The X-ray crystal structure of (2*S*)-**6**·trypsin (vide infra) suggests that this difference is associated with adverse steric interactions between inhibitor molecule **20** and Gly-216/Trp-215 of the β-sheet of tryptase. Proline and azetidine-2-carboxylic acid substitution at the P2 position (S2 subsite) were equally effective, cf. **12** with **16**; however, sp^2-hybridized proline ring carbons decreased affinity: cf. **12** with **15** and (2*S*)-**6** with **14**. Substitution of proline with a *trans*-4-hydroxyproline gave equivalent potency: cf. **6** with **12**.

Selectivity data for (2*S*)-**6** relative to five other serine proteases are presented in Table 2, along with data for reference inhibitor **2**. For comparison, published results for inhibitor **1** are also offered. These enzyme assays were conducted in the absence of any added zinc, conditions which can dramatically increase the serine protease affinity of **2** and its analogues.[17] It is noteworthy that (2*S*)-**6** is a considerably more potent tryptase inhibitor than **2** (K_i value of 10 vs 140 nM), which may be related to (2*S*)-**6** having a better fit in the enzyme active site or forming a covalent hemiacetal with the Ser-195 hydroxyl of tryptase (see X-ray section). Neither (2*S*)-**6** nor **2** was selective for tryptase over trypsin. Compound (2*S*)-**6** was much more selective over thrombin than **2** (31 000 vs 32), and it was also significantly more selective than **2** vs plasma kallikrein (32 vs 0.7),

Chart 2. Analogues of (2*S*)-**6**

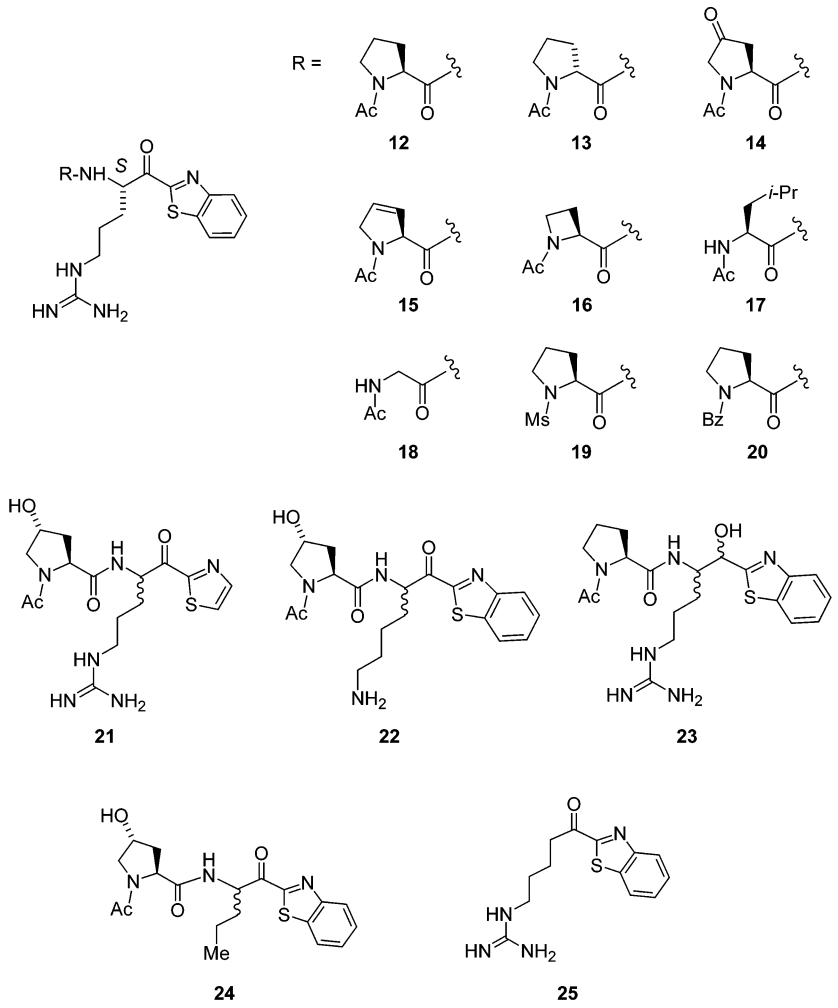

Table 2. Inhibition of Tryptase Relative to Other Serine Proteases

	K_i (nM)[a]	selectivity (K_i other/K_i tryptase)[b]					
compd	tryptase	trypsin	kallikrein	uPA	plasmin	thrombin	factor Xa
(2*S*)-**6**[c]	10 ± 3 (7)	0.8	32	220	810	31 000	5700
APC-366 (**1**)[d]	330	0.5	>3000	–[e]	>3000	1.3	–[e]
Babim (**2**)[f]	140 ± 20 (16)	1.3	0.7	7.5	20[g]	32[g]	10

[a] K_i values (mean ± standard error) are given for tryptase inhibition; the number of experiments (*N*) is given in parentheses. [b] Selectivity is defined as the ratio of the K_i value of the serine protease over the K_i value for tryptase; uPA = urokinase-type plasminogen activator. For the original K_i data, see the paragraph at the end of this paper regarding Supporting Information. All K_i data were obtained without the addition of exogenous zinc (refs 5b and 17). [c] Determined for the trifluoroacetate hydrate (1.2 TFA, 1.4 water). [d] The tryptase K_i value and the selectivities are derived from ref 5a. [e] Not reported. [f] Reference tryptase inhibitor, the tryptase K_i of which decreased to 0.48 ± 0.17 nM ($N = 3$) in the presence of 80 μM $ZnCl_2$ (refs 5b and 17). [g] Selectivity was calculated from the published plasmin and thrombin K_i data (ref 6c).

urokinase plasminogen activator (220 vs 7.5), and plasmin (810 vs 20).

X-ray Crystal Structure of (2*S*)-6·Trypsin. Since our attempts to obtain diffracting crystals of (2*S*)-**6**·tryptase were unsuccessful, the X-ray crystal structure of a complex between (2*S*)-**6** and bovine pancreatic β-trypsin was determined (Figure 1).[18,19] Crystals of the (2*S*)-**6**·trypsin complex, trigonal space group $P3_121$, were grown by the hanging-drop technique under the same conditions as reported for (2*S*)-**5**.[10] Diffraction data were collected at −170 °C and processed to a resolution of 1.9 Å.[19a] The completeness of the data at this resolution was 98.6% and the final refinement had convergence at $R = 0.175$ and $R_{free} = 0.206$ with 225 water molecules.

The overall structure of (2*S*)-**6**·trypsin (Figures 1 and 2) is analogous to that of (2*S*)-**5**·trypsin, although there are some significant differences. As expected, both inhibitors form a hemiketal adduct between the ketone carbonyl and the Ser-195 hydroxyl, a hydrogen bond between the benzothiazole nitrogen and Nϵ of His-57, and a hydrogen bond between the P1 amide carbonyl and the nitrogen of Gln-192. In the (2*S*)-**6**·trypsin complex, these bond lengths are 1.45, 3.16, and 2.71 Å, respectively. By contrast to (2*S*)-**5**·trypsin, the inhibitor in (2*S*)-**6**·trypsin extends more deeply into the S2 domain presumably because of additional hydrogen bonding involving the acetyl group of (2*S*)-**6**. Even though the hydroxyl group of (2*S*)-**6** is a participant in

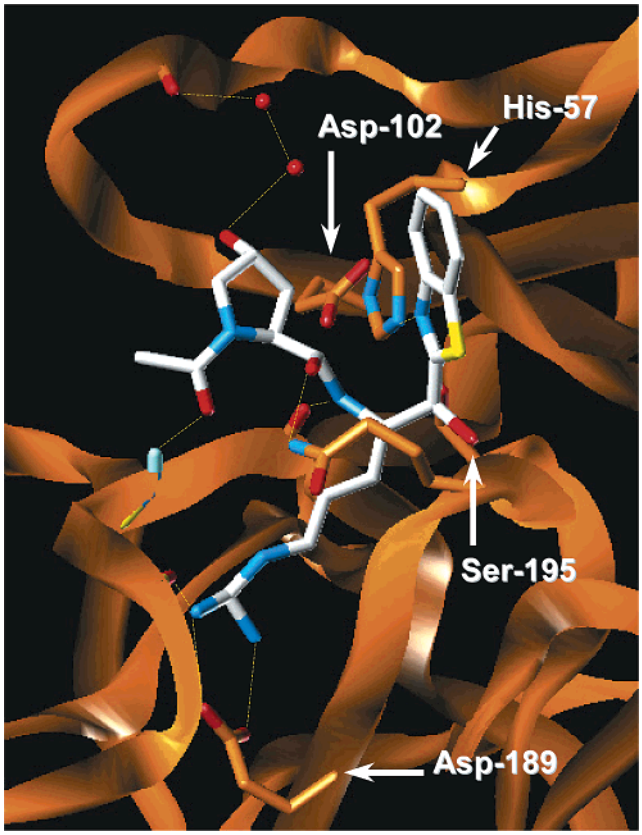

Figure 1. View of (2*S*)-**6** (a generally white stick model with the heteroatoms represented by standard colors) bound in the active site of trypsin (orange ribbon bearing specific amino acid side chains).

a hydrogen bond network with several water molecules, this aspect does not lead to a significant increase in either trypsin or tryptase affinity (Table 1; cf. **6** with **12**). Specifically, the acetyl carbonyl of (2*S*)-**6** forms a hydrogen bond with the nitrogen of Gly-216 (length = 3.01 Å), and the hydroxyl group of (2*S*)-**6** forms a hydrogen bond network that links two water molecules to the carbonyl group of Ser-96 (lengths = 2.82, 2.64, and 2.74 Å). Consequently, the minimum interatomic distance between the benzothiazole phenyl ring and the Cys-42/Cys-58 disulfide bond is increased by 1.07 Å, indicating a significant decrease in van der Waals interactions in (2*S*)-**6**·trypsin relative to the (2*S*)-**5**·trypsin (5.37 Å vs 4.30 Å). In addition, the plane of the proline ring of (2*S*)-**6** is essentially parallel to the Ser-213 through Ser-217 β-strand, whereas the cyclopentyl ring of (2*S*)-**5** is angled about 60° from the β-strand. This change in ring orientation results in a decrease in van der Waals interactions, which is reflected by a 1.05 Å increase in the minimum interatomic distance between the Leu-99 methyl groups and the proline ring of (2*S*)-**6** relative to the cyclopentyl ring of (2*S*)-**5** (4.32 Å vs 3.27 Å, respectively).

Antiasthmatic Activity of 6. We evaluated **6** (2*R*,2*S* mixture, RWJ-58643, HCl salt), for in vivo efficacy in conscious, antigen-sensitized allergic sheep, which is a well characterized asthma model.[20] The inhibitor was administered by aerosol as a total dose of 9 mg, twice a day, for three consecutive days, and as a single, 9-mg dose on day 4, 2 h prior to antigen challenge (Figure 3). As depicted in panel A of Figure 3, inhaled antigen caused the expected airway resistance responses under control conditions (no drug treatment). Immediately after challenge there was a mean 300% increase over baseline in specific lung resistance (SR_L; early response). SR_L returned to baseline between 2 and 6 h post challenge and then increased again between 6 and 8 h post challenge to 100% over baseline (late response). When these same sheep were treated with **6**, however, the early response was inhibited by 70−75% and the late response was completely blocked. Panel B of Figure 3 depicts the post antigen-induced changes in airway sensitivity. Prior to antigen challenge (BSL), the dose of carbachol that elicited a 400% increase in SR_L (PC_{400}) was the same for both the control experiments and the experiments with **6**. Twenty-four hours after antigen challenge, the sheep in the control group developed airway hyper-responsiveness as evidenced by the 2-fold decrease in the PC_{400}. When these sheep were treated with **6**, this airway hyper-responsiveness was completely blocked, i.e., the post-challenge PC_{400} value was not different from the preantigen value.

Conclusion

We identified a series of the potent, reversible, low-molecular-weight tryptase inhibitors, represented by **5** and (2*S*)-**6**. The compounds of interest are transition-state mimetics that feature a heterocycle-activated ketone group, which can form a hemiketal with the γ-oxygen of Ser-195 and a hydrogen bond with the ϵ-nitrogen of His-57. An X-ray crystal structure of (2*S*)-**6** bound to bovine trypsin at 1.9-Å resolution depicted these key interactions. In comparing the structure of (2*S*)-**6**·trypsin with (2*S*)-**5**·trypsin,[10] (2*S*)-**6** extends more deeply into the S2 domain of the enzyme, possibly because of the hydrogen-bonding interaction between the acetyl group of (2*S*)-**6** and Gly-216 of trypsin. Since there is a high degree of homology between the active site cavities of tryptase and trypsin, a similar hydrogen-bonding interaction could occur in the (2*S*)-**6**·tryptase complex. Given that **6** is ca. four times more potent than **5** as a tryptase inhibitor, the introduction of this planned interaction is an example of effective structure-based drug design. The incorporation of a proline hydroxyl into **12**, to obtain **6**, did not lead to increased tryptase affinity, nor to better selectivity vs trypsin. Hence, the intended hydrogen bond interaction between the hydroxyl of **6** and the amide side chain of Gln-98 of tryptase is probably not formed.

In our thrombin inhibitor studies,[8a] the 2-benzothiazole derivative was nearly 20 times more potent than the corresponding 2-thiazole derivative. In that case, we noted an aromatic stacking interaction between the benzene ring of the benzothiazole and Trp-60D. For tryptase inhibition, we found that benzothiazole **6** is eight times more potent than thiazole **21**. Here, the benzothiazole group may be more effective than the thiazole because of increased ketone electrophilicity and/or increased electron density on the ring nitrogen in the former.[21] Additionally, the benzene ring of the benzothiazole may participate in a hydrophobic interaction with the Cys-42/Cys-58 disulfide bond of tryptase (cf. Figure 2).

In the well-characterized sheep model of asthma, aerosol administration of **6** strongly blunted the early

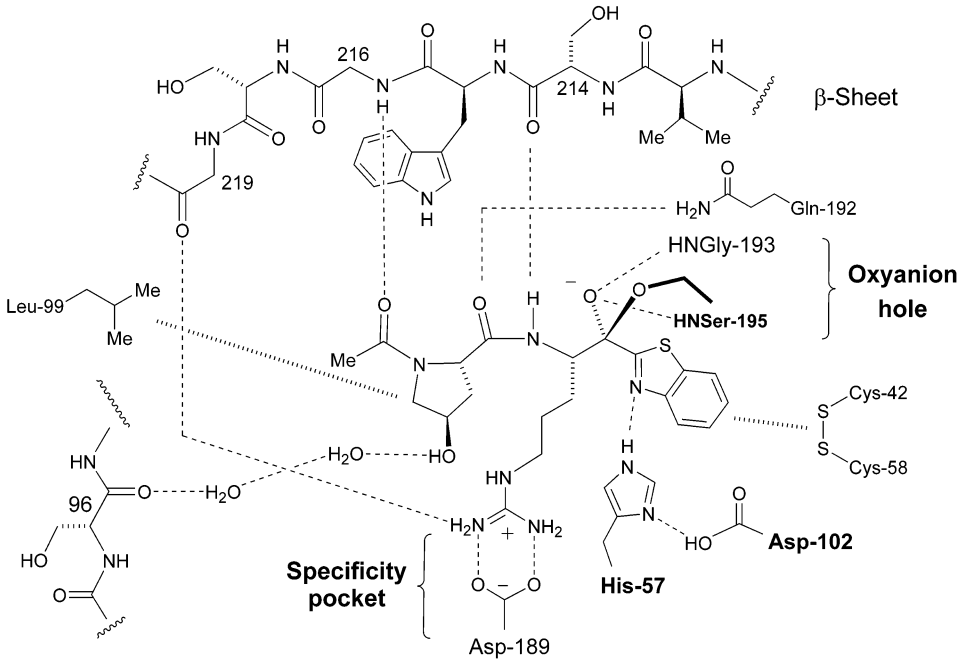

Figure 2. Schematic representing the interactions of (2*S*)-**6** with trypsin.

response (70−75% blockade) and completely abolished the late response and airway hyper-responsiveness. These noteworthy results reflect on the potential of this compound for the treatment of asthma in humans, and **6** has advanced into clinical trials.

Experimental Section

General Information. ^{1}H NMR spectra were acquired at 300.14 MHz on a Bruker Avance-300 spectrometer in CD_3OD unless indicated otherwise, using Me_4Si as an internal standard. NMR abbreviations used: s, singlet; d, doublet; dd, doublet of doublets; t, triplet; m, multiplet; br, broad; ov, overlapping. ^{13}C NMR spectra were acquired 125.76 MHz at 40 °C on a Bruker Avance-500 spectrometer. HPLC analyses were performed on a Hewlett-Packard Series 1100 HPLC instrument eluting with a gradient of water/MeCN/CF_3CO_2H (10:90:0.2 to 90:10:0.2) over 4 min with a flow rate of 0.75 mL/min on a Kromasil C18 column (50 × 2.0 mm; 3.5 μm particle size) or on a Supelcosil ABZ+Plus column (50 × 2.1 mm; 3.0 μm particle size) at 32 °C. Signals were recorded simultaneously at 220, 254, and 305 nm with a diode array detector; purity is reported for the 220-nm signal. Normal-phase preparative chromatography was performed on an Isco Combiflash Separation System Sg 100c equipped with a Biotage FLASH Si 40M silica gel cartridge (KP-Sil Silica, 32−63 μm, 60 Å; 4 × 15 cm) eluting at 35 mL/min with detection at 254 nm. Reverse-phase preparative chromatography was performed on a Waters Delta-Prep 3000 HPLC equipped with 3 PrepPak reverse-phase cartridges connected in series (Bondapak C-18; 40 × 300 mm; 15−20 μm, 125 Å) eluting at 40 mL/min with detection at 220 nm unless noted otherwise. Melting points were determined on a Thomas-Hoover apparatus calibrated with a set of melting point standards. Optical rotations were measured on a Perkin-Elmer 241 polarimeter. Electrospray (ES) mass spectra were obtained on a Micromass Platform LC single quadrupole mass spectrometer in the positive mode. Accurate mass determination was performed on an Autospec E high-resolution magnetic sector mass spectrometer tuned to a resolution of 6K; the ions were produced in a fast atom bombardment source at 8 kV. Linear voltage scans were collected to include the sample ion and two poly(ethylene glycol) ions, which were used as internal reference standards. Elemental analysis and Karl Fischer water analysis were determined by Robertson Microlit Laboratories, Inc., Madison, NJ.

***N*-[4-[(Aminoiminomethyl)amino]-1-(2-benzothiazolylcarbonyl)butyl]cyclopentanecarboxamide (5).** Compound **10** (0.676 g, 1.0 mmol) and cyclopentanecarboxylic acid (0.285 g, 2.5 mmol) were coupled, oxidized, and deprotected to give **5** according to methodology described for **6**. Crude **5** was purified by reverse phase HPLC (water/MeCN/CF_3CO_2H, 30:20:0.1). The fractions containing the desired product were combined and lyophilized to afford **5** as a white solid (0.336 g, 62%) with a HPLC purity of 99%. The ratio of 2*S*/2*R* arginine epimers was determined to be 1.7:1 by ^{13}C NMR via the ratio of the peak integrals at 122.32 and 122.16 ppm, respectively, in the presence of 4.3 mol equiv of (*R*)-(−)-2,2,2-trifluoro-1-(9-anthryl)ethanol in $CDCl_3$ at 40 °C; mp 60−70 °C; $[\alpha]^{20}_D$ +5.1° (*c* 0.68, MeOH); ^{1}H NMR ($CDCl_3$) δ 1.40−2.10 (ov m, 12H), 2.10−2.30 (br m, 1H), 2.55−2.80 (br m, 1H), 2.80−3.15 (br m, 1H), 3.15−3.40 (br m, 1H), 3.60−3.90 (br m, 1H), 5.70−5.90 (m, 1H), 6.80−7.30 (br s, 6H), 6.92 (d, 1H, J = 6.9 Hz), 7.50−7.70 (m, 2H), 7.98 (d, 1H, J = 7.3 Hz), 8.19 (d, 1H, J = 6.9 Hz), 8.20−8.30 (br s, 1H); ^{13}C NMR ($CDCl_3$) δ 25.10, 25.85, 25.90, 30.45, 30.63, 30.97, 40.64, 45.66, 54.15, 122.36, 125.87, 127.44, 128.35, 137.26, 153.42, 157.59, 163.21, 178.18, 192.68; MS (ES) *m*/*z* 388 $(MH)^+$. Anal. ($C_{19}H_{25}N_5O_2S\cdot1.25CF_3CO_2H\cdot0.75H_2O$) C, H, N, F, H_2O.

(2*S*,4*R*)-1-Acetyl-*N*-[4-[(aminoiminomethyl)amino]-1-(2-benzothiazolylcarbonyl)butyl]-4-hydroxy-2-pyrrolidinecarboxamide (6). Acetyl chloride (3.3 mL, 46 mmol) was added dropwise to a solution of *O*-benzyl-L-4-*trans*-hydroxyproline methyl ester hydrochloride (**7**; 12.5 g, 46 mmol) and triethylamine (6.4 mL, 46 mmol) in pyridine (150 mL) at 0 °C while stirring under argon (Scheme 1). The reaction mixture was stirred for 30 min at 0 °C then slowly warmed to room temperature over 16 h. The reaction mixture was concentrated in vacuo, diluted with CH_2Cl_2, washed with 1 N HCl (3×), 10% aqueous Na_2CO_3, saturated aqueous $NaHCO_3$, and brine, dried ($MgSO_4$), and concentrated in vacuo. The residue was purified by chromatography on silica gel (CH_2Cl_2/MeOH, 49:1) to give 7.12 g (55%) of Ac-Hyp(OBzl)-OMe as an oil. This oil (5.38 g, 19.4 mmol) was dissolved in tetrahydrofuran (260 mL), cooled to 0 °C, treated dropwise with 0.15 M LiOH (260 mL, 39 mmol), and stirred for 30 min. The reaction mixture was concentrated in vacuo, acidified with 1 N HCl, and extracted three times with ethyl acetate. The combined organic extracts were dried (Na_2SO_4) and concentrated in vacuo to give 3.79 g (73%) of *trans*-1-acetyl-4-benzyloxy-L-proline (**8**) as a white solid.

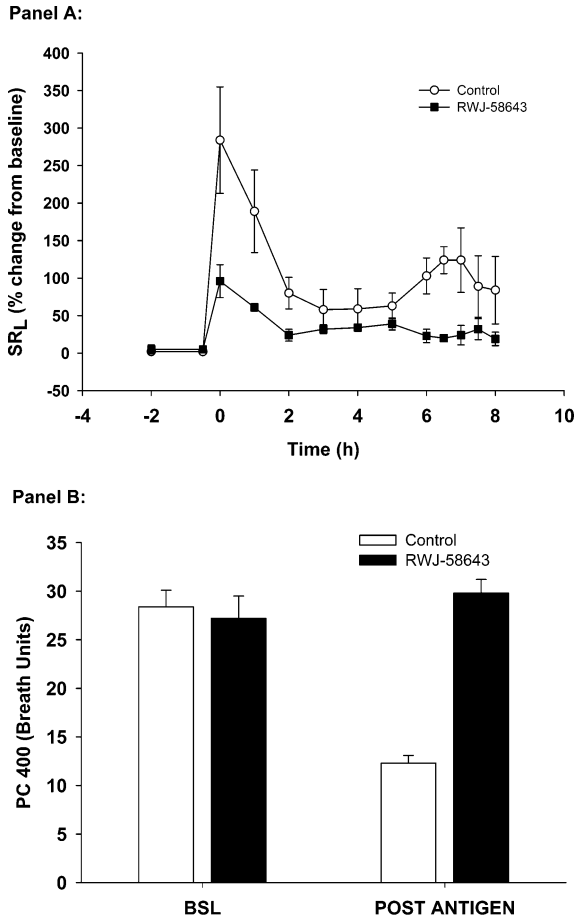

Figure 3. Administration of **6** to conscious allergic sheep by aerosol in a multiple-dosing protocol (see text). Panel A: Increase in specific lung resistance (SR_L); (○) control animals; (■) animals treated with **6** (RWJ-58643). Panel B: Change in airway responsiveness at baseline (BSL) and 24 h following antigen challenge (post antigen); open bar, control experiments; filled bar, treatment with **6** (RWJ-58643). Values are given as the mean ± standard error for $N = 4$.

Compound **10** (12.12 g, 0.027 mol), **8** (7.13 g, 0.027 mol), and 1-hydroxybenzotriazole hydrate (HOBT; 9.16 g, 0.068 mol) were combined in *N*,*N*-dimethylformamide (DMF, 270 mL) and treated with 1,3-dicyclohexylcarbodiimide (DCC; 13.99 g, 0.068 mol). The reaction was stirred under argon at room temperature for 18 h and filtered. The filtrate was diluted with water (ca. 800 mL), extracted with ethyl acetate (3×), washed with water, dried (Na_2SO_4), and concentrated in vacuo. The residue was purified by chromatography on silica gel (CH_2Cl_2/MeOH, 19:1) to afford 15.0 g (80%) of **11** as a white solid.

The Dess−Martin periodinane (18.7 g, 0.044 mol) was added to a solution of **11** (14.9 g, 0.022 mol) in CH_2Cl_2 (220 mL) under argon at room temperature and stirred for 1 h. The reaction mixture was quenched with a solution containing 20% $Na_2S_2O_3$ (w/w) in saturated aqueous $NaHCO_3$, and the mixture was allowed to epimerize by stirring at 23 °C for 2 h. The organic layer was separated, washed with brine, dried (Na_2SO_4), and concentrated in vacuo to furnish a white solid. This solid was dissolved in anhydrous anisole (ca. 12 mL) in a Teflon reaction vessel, placed on a HF apparatus, and cooled to −78 °C. Anhydrous HF (ca. 38 mL) was condensed into the reaction vessel, and the reaction was warmed to 0 °C. The reaction was stirred at 0 °C for 6 h, concentrated in vacuo, and triturated with ethyl ether (3×) to furnish a white solid. This solid was purified by reverse-phase HPLC eluting with a gradient of water/acetonitrile/trifluoroacetic acid (90:10:0.2 to 70:30:0.2) on six PrepPak cartridges connected in series (Bondapak C-18; 40 × 300 mm; 15−20 μm, 125 Å) eluting at 40 mL/min over 60 min. The fractions containing the both diastereomers of **6** were combined and lyophilized to give **6** (2*S*/2*R* = 1.1:1) as the trifluoroacetate (TFA) salt, which was converted to the HCl salt by dissolving the TFA salt into 0.1 N HCl and concentrating in vacuo three times in succession. The resulting glass was dissolved in water and lyophilized twice to afford 7.9 g (63%) of the HCl salt of **6** as a light yellow solid with 95% purity by HPLC and an L/D-arginine epimeric ratio of 1.2:1 by HPLC; ^{1}H NMR δ 1.50−2.40 (ov m, 9H), 3.10−3.90 (ov m, 3H), 4.22−4.90 (ov m, 3H), 5.52−5.63 (m, 0.4H), 5.63−5.74 (m, 0.6H), 7.50−7.80 (m, 2H), 8.00−8.28 (m, 2H); MS (ES) *m*/*z* 447 $(MH)^+$. Anal. ($C_{20}H_{26}N_6O_4S\cdot2.50HCl\cdot2.2H_2O$) C, H, N, S, H_2O.

(2*S*,4*R*)-1-Acetyl-*N*-[(1*R*)-4-[(aminoiminomethyl)amino]-1-(2-benzothiazolylcarbonyl)butyl]-4-hydroxy-2-pyrrolidinecarboxamide [(2*R*)-6]. The protocol for the synthesis of **6** was repeated, and the product was purified by reverse phase HPLC, eluting with a gradient of water/MeCN/CF_3CO_2H (90:10:0.2 to 70:30:0.2) over 60 min. The fractions containing the earlier eluting diastereomer were combined and lyophilized to give (2*R*)-**6** as a TFA salt. This material (160 mg, 0.258 mmol) was dissolved into 3.8 mL of warm MeCN/MeOH (3.8:1) and treated with a solution of HNO_3 (23 mg, 0.258 mmol) in MeCN. The clear solution was concentrated under a stream of nitrogen to yield an oil, which was dissolved in water and lyophilized to give (2*R*)-**6** as a white hygroscopic solid. ^{1}H NMR δ 1.60−2.00 (ov m, 4H), 2.08 (s, 3H), 2.10−2.30 (m, 2H), 3.45−3.60 (m, 1H), 3.74 (dd, 1H, J = 4.4, 11.1 Hz), 4.35−4.40 (m, 1H), 4.53 (t, 1H, J = 8.2 Hz), 5.59 (dd, 1H, J = 3.7, 9.2 Hz), 7.55−7.70 (m, 2H), 8.08 (d, 1H, J = 7.4 Hz), 8.18 (d, 1H, J = 6.8); MS (ES) *m*/*z* 447 $(MH)^+$. Anal. ($C_{20}H_{26}N_6O_4S\cdot HNO_3\cdot0.3CF_3CO_2H\cdot1.3H_2O$) C, H, N, F, S, H_2O.

(2*S*,4*R*)-1-Acetyl-*N*-[(1*S*)-4-[(aminoiminomethyl)amino]-1-(2-benzothiazolylcarbonyl)butyl]-4-hydroxy-2-pyrrolidinecarboxamide [(2*S*)-6]. The protocol for **6** was repeated, except the Dess−Martin oxidation was processed immediately after quenching with 20% $Na_2S_2O_3$ (w/w) in saturated aqueous $NaHCO_3$ to minimize epimerization. The product was purified by reverse-phase HPLC (water/MeCN/CF_3CO_2H, 90:10:0.2 to 70:30:0.2) over 60 min, and the fractions containing the slower-eluting diastereomer were combined and lyophilized to give 1.5 g of (2*S*)-**6** as a TFA salt. The purified salt (1.5 g, 2.42 mmol) was dissolved into warm MeCN with a small amount of MeOH and treated with a solution of HNO_3 (0.21 g, 2.42 mmol) in MeCN. The white crystalline solid that formed on cooling was washed with MeCN and dried in vacuo to give (2*S*)-**6** (1.04 g, 84%) as a nitrate salt, mp 174.5−176.5 °C; ^{1}H NMR δ 1.50−2.08 (ov m, 4H), 2.10 (s, 3H), 2.12−2.30 (m, 2H), 3.54 (d, 1H, J = 11.1 Hz), 3.76 (dd, 1H, J = 4.1, 11.1 Hz), 4.40−4.49 (m, 1H), 4.57 (t, 1H, J = 8.1 Hz), 5.70−5.82 (m, 1H), 7.55−7.70 (m, 2H), 8.08 (d, 1H, J = 7.4 Hz), 8.18 (d, 1H, J = 6.8); MS (ES) *m*/*z* 447 $(MH)^+$. Anal. ($C_{20}H_{26}N_6O_4S\cdot HNO_3\cdot0.04H_2O$) C, H, N, S, H_2O.

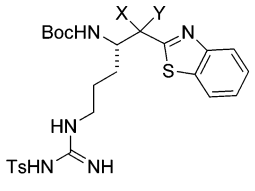

26 X/Y = O
27 X/Y = H, OH

(4*S*)-*N*-[[[4-Amino-5-(2-benzothiazolyl)-5-hydroxypentyl]amino]iminomethyl]-4-methylbenzenesulfonamide (10). Butyllithium in hexanes (2.5 M) (68 mL, 170 mmol) was added dropwise to a stirred solution of distilled benzothiazole (56.8 g, 420 mmol) in dry tetrahydrofuran (600 mL) at 78 °C under argon at a rate that kept the reaction temperature below −64 °C. Upon completion of addition, the reaction mixture was stirred for 30 min at −70 °C, and a solution of **9**[13] (20.0 g, 42.4 mmol) in dry tetrahydrofuran (500 mL) was added at a rate to maintain the reaction temperature below −70 °C. The resulting mixture was slowly warmed to room temperature over 2 h and quenched with saturated aqueous NH_4Cl (250

mL). The resulting organic layer was separated, washed with brine, dried (Na_2SO_4), and concentrated in vacuo. The residue was triturated thrice with hexane and purified by chromatography on silica gel (ethyl acetate/hexane, 3:2) to furnish ketone **26** as an amber solid.

$NaBH_4$ (3.7 g, 0.097 mol) was added portionwise to a stirred solution of **26** (17.8 g, 0.033 mmol) in dry methanol (165 mL) under argon at −30 °C. After 3 h, the reaction was quenched with acetone (30 mL) and concentrated in vacuo. The residue was dissolved in CH_2Cl_2, washed sequentially with 10% aqueous citric acid, water, and brine, dried (Na_2SO_4), and concentrated in vacuo to give alcohol **27** as a yellow solid.

Compound **27** (1.0 g, 1.8 mmol) was treated with trifluoroacetic acid/CH_2Cl_2 (1:1 v/v; 50 mL) and stirred at 23 °C for 2 h. The reaction mixture was concentrated in vacuo, dissolved in ethyl acetate, and extracted with a 1:1 mixture (v/v) of brine and 10% aqueous Na_2CO_3. The organic layer was extracted once with brine, dried (Na_2SO_4), and concentrated in vacuo to furnish **10** as a yellow solid with a HPLC purity of 97%; ^{1}H NMR δ 1.10−1.80 (ov m, 4H), 2.36 (s, 3H), 2.90−3.40 (ov m, 3H), 4.83 (d, 0.5 H, J = 4.4 Hz), 4.91 (d, 0.5 H, J = 4.6 Hz), 7.25 (d, 2H, J = 7.3 Hz), 7.33−7.55 (ov m, 2H), 7.60−7.70 (m, 2H), 7.94 (d, 1H, J = 8.4 Hz), 7.98 (d, 1H, J = 7.8 Hz); MS (ES) m/z 448 $(MH)^+$.

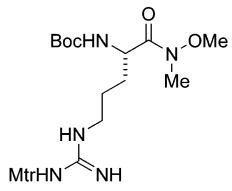

28

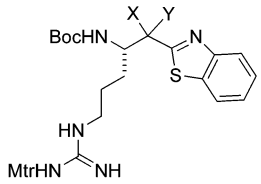

29 X/Y = O
30 X/Y = H, OH

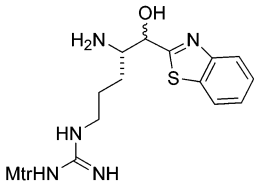

31

(2*S*)-1-Acetyl-*N*-[4-[(aminoiminomethyl)amino]-1-(2-benzothiazolylcarbonyl)butyl]-2-pyrrolidinecarboxamide (12). Benzotriazol-1-yloxytris(dimethylamino)phosphonium hexafluorophosphate (BOP reagent; 25.0 g, 56 mmol) was added in one portion to a stirring solution of *N*-α-*t*-Boc-N^G-(4-methoxy-2,3,6-trimethylbenzenesulfonyl)-L-arginine (Boc-Arg-(Mtr)-OH; 24.96 g, 51.3 mmol), *N*,*O*-dimethylhydroxylamine hydrochloride (7.6 g, 56 mmol), and triethylamine (22 mL, 154 mmol) in dry DMF (100 mL) under argon at 0 °C. The reaction mixture was allowed to slowly warm to room temperature over 2 h, filtered through diatomaceous earth, and concentrated in vacuo. The residue was dissolved in ethyl acetate, washed sequentially with H_2O (three times), 1 M $KHSO_4$, saturated aqueous $NaHCO_3$, and brine, dried (Na_2SO_4), and concentrated in vacuo. The residue was purified by chromatography on silica gel (ethyl acetate/CH_2Cl_2, 3:1) to give **28**[14d] as a white solid.

Butyllithium in hexanes(2.5 M) (164 mL, 410 mmol) was added dropwise at −78 °C under argon to a stirred solution of benzothiazole (69.2 g, 512 mmol) in dry tetrahydrofuran (1 L) at a rate that kept the reaction temperature below −64 °C. On completion of addition, the reaction mixture was stirred for 30 min at −70 °C, and a solution of **28** (27.11 g, 51.2 mmol) in dry tetrahydrofuran (200 mL) was added at a rate that maintained the temperature below −70 °C. The reaction was stirred for 15 min, quenched with saturated aqueous NH_4Cl (500 mL), and stirred for 16 h at 23 °C. The resulting organic layer was separated, diluted with ethyl acetate, washed with water and brine, dried (Na_2SO_4), and concentrated in vacuo. The thick syrupy residue was triturated with hexanes (3×) and purified by chromatography on silica gel (CH_2Cl_2/ethyl acetate, 7:3) to afford **29** as a light yellow solid.

$NaBH_4$ (4.9 g, 129 mmol) was added portionwise to a stirring solution of **29** (15.0 g, 27.4 mmol) in dry methanol (200 mL) under argon at 0 °C. The reaction mixture was slowly warmed to 23 °C over 1 h, quenched with acetone (30 mL), and concentrated in vacuo. The residue was dissolved in ethyl acetate, washed with water (2×) and brine, dried (Na_2SO_4), and concentrated in vacuo to give **30** as a yellow solid.

p-Toluenesulfonic acid monohydrate (TsOH·H_2O) was added at 23 °C to solution of **30** (1.0 g, 1.8 mmol) in CH_2Cl_2 (20 mL) until the solution was saturated. The reaction was stirred at 23 °C for 6 h, diluted with ethyl acetate, extracted twice with a 1:1 mixture (v/v) of brine and 10% aqueous Na_2CO_3, dried (Na_2SO_4), and concentrated in vacuo to give **31** as a yellow solid.

Compound **31** and *N*-acetyl-L-proline was coupled with DCC and oxidized with the Dess−Martin periodinane according to methodology described for **6**. The resulting ketone (0.040 g, 0.062 mmol) was dissolved in trifluoroacetic acid (6 mL), stirred at 23 °C for 6 h, and concentrated in vacuo to give crude **12**, which was purified by reverse-phase HPLC with water/MeCN/CF_3CO_2H (90:10:0.2 to 60:40:0.2) over 60 min to give **12** (0.010 g, 27%) as a white solid with 96% purity by HPLC and an L/D-arginine ratio of 1.0:1 by ^{1}H NMR; ^{1}H NMR δ 1.8−2.0 (ov m, 6H), 2.11 (s, 3H), 2.12−2.40 (br m, 2H), 3.20−3.75 (ov m, 4H), 4.35−4.50 (m, 1H), 5.50−5.65 (m, 0.5H), 5.65−5.80 (m, 0.5H), 7.50−7.70 (m, 2H), 8.10 (d, 1H, J = 7.2 Hz), 8.21 (d, 1H, J = 6.9 Hz); MS (ES) m/z 431 $(MH)^+$. Anal. ($C_{20}H_{26}N_6O_3S$·1.30CF_3CO_2H·1.40H_2O) C, H, N, F, H_2O.

(2*R*)-1-Acetyl-*N*-[4-[(aminoiminomethyl)amino]-1-(2-benzothiazolylcarbonyl)butyl]-2-pyrrolidinecarboxamide (13). Compound **10** (1.00 g, 1.83 mmol) and acetyl-D-proline (0.426 g, 2.7 mmol) were converted crude **13** according to methodology described for **6**. The crude material was purified by reverse-phase HPLC eluting with a gradient of water/MeCN/CF_3CO_2H (90:10:0.2 to 60:40:0.2) over 60 min to give **13** (37 mg) as a white solid with a HPLC purity of 95% and an L/D-arginine epimeric ratio of 1:2.5 by ^{1}H NMR; ^{1}H NMR δ 1.60−2.05 (ov m, 6H), 2.08 (s, 3H), 2.12−2.30 (br m, 2H), 3.10−3.3 (ov m, 2H), 3.46−3.72 (ov m, 2H), 4.40−4.45 (m, 0.7H), 4.45−4.55 (m, 0.3H), 5.58−5.65 (m, 0.7H), 5.65−5.76 (m, 0.3H), 7.55−7.70 (m, 2H), 8.10 (d, 1H, J = 7.2 Hz), 8.21 (d, 1H, J = 6.9 Hz); MS (ES) m/z 431 $(MH)^+$. Anal. ($C_{20}H_{26}N_6O_3S$·1.07CF_3CO_2H·1.13H_2O) C, H, N, F, H_2O.

(2*S*)-1-Acetyl-*N*-[4-[(aminoiminomethyl)amino]-1-(2-benzothiazolylcarbonyl)butyl]-4-oxo-2-pyrrolidinecarboxamide (14). Compound **31** (0.67 g, 1.32 mmol) and (4*R*)-1-acetyl-4-hydroxy-L-proline (0.23 g, 1.32 mmol) were converted to crude **14** according to methodology described for **12** with the exception that 4 mol equiv of the Dess−Martin periodinane was used instead of 2 mol equiv. The crude material was purified by reverse-phase HPLC eluting with a gradient of water/MeCN/CF_3CO_2H (90:10:0.2 to 70:40:0.2) over 60 min to give **14** (8 mg) as a white solid with 99% purity and an L/D-arginine epimeric ratio of 8.4:1 by HPLC; ^{1}H NMR δ 1.70−1.90 (br m, 3H), 2.09 (s, 0.3H), 2.11 (s, 2.7H), 2.12−2.30 (b m, 1H), 2.53 (dd, 1 H, J = 3.4, 18.7 Hz), 3.00 (dd 1H, J = 10.2, 18.7 Hz), 3.10−3.30 (m, 2H), 4.10 (dd, 2H, J = 7.8, 16.7 Hz), 4.80−5.05 (m, 1H), 5.65−5.80 (b m, 1H), 7.50−7.70 (m, 2H), 8.17 (d, 1H, J = 7.2 Hz), 8.21 (d, 1H, J = 6.6 Hz); MS (ES) m/z 445 $(MH)^+$. HRMS (FAB) m/z 445.1662 (445.1658 calcd for $C_{20}H_{24}N_6O_4S + H^+$).

(2*S*)-1-Acetyl-*N*-[4-[(aminoiminomethyl)amino]-1-(2-benzothiazolylcarbonyl)butyl]-2,5-dihydro-1*H*-pyrrole-2-carboxamide (15). 3,4-Dehydro-L-proline methyl ester hydrochloride (0.50 g, 3.06 mmol, triethylamine (1.0 mL, 7.2 mmol), and acetyl chloride (0.22 mL, 3.1 mmol) were added to CH_2Cl_2 (50 mL) with stirring under argon at 5 °C. The reaction mixture was slowly warmed to 23 °C, stirred for 18 h, and concentrated in vacuo. The residue was dissolve in 10 mL of tetrahydrofuran/water (1:1), treated with LiOH·H_2O (0.13 g, 3.06 mmol), and stirred for 18 h. The mixture was concentrated

in vacuo and lyophilized. The resulting residue and **26** (1.47 g, 2.91 mmol) were converted into crude **15** according to methodology described for **12** with the exception that 4 mol equiv of the Dess−Martin periodinane was used instead of 2 mol equiv. The crude material was purified by reverse-phase HPLC with water/MeCN/CF_3CO_2H (90:10:0.2 to 70:40:0.2) over 60 min to give **15** (125 mg) as a white solid with 99% purity and an L/D-arginine epimeric ratio of 1.5:1 by HPLC; ^{1}H NMR δ 1.70−1.93 (br m, 3H), 2.08 (s, 1.2H), 2.11 (s, 1.8H), 2.12−2.33 (m, 1H), 3.21−3.33 (m, 2H), 4.20−4.45 (m, 2H), 5.14−5.30 (m, 1H), 5.60−5.90 (m, 2H), 5.95−6.10 (m, 1H), 7.59−7.72 (m, 2H), 8.10 (d, 1H, J = 7.4 Hz), 8.20 (d, 1H, 6.8 Hz); MS (ES) m/z 429 $(MH)^+$. Anal. ($C_{20}H_{24}N_6O_3S\cdot1.22CF_3CO_2H\cdot0.84H_2O$) C, H, N, F, H_2O.

(2*S*)-1-Acetyl-*N*-[4-[(aminoiminomethyl)amino]-1-(2-benzothiazolylcarbonyl)butyl]-2-azetidinecarboxamide (16). Compound **31** (0.55 g, 1.1 mmol) and (*S*)-2-azetidinecarboxylic (0.26 g, 1.8 mmol) were converted to crude **16** according to methodology described for **12**. The crude material was purified by reverse-phase HPLC with water/MeCN/CF_3CO_2H (90:10:0.2 to 70:40:0.2) over 60 min to give **16** (125 mg) as a white solid with 99.9% purity by HPLC and an L/D-arginine epimeric ratio of 2.5:1 by ^{1}H NMR; ^{1}H NMR δ 1.70−1.89 (m, 3H), 1.90 (s, 2.1H), 1.94 (s, 0.9H), 2.10−2.36 (m, 2H), 2.40−2.70 (m, 1H), 3.22−3.35 (m, 2H), 4.10−4.20 (m, 2H), 4.95−5.05 (m, 1H), 5.60−5.82 (m, 1H), 7.55−7.70 (m, 2H), 8.13 (d, 1H, J = 7.5 Hz), 8.23 (d, 1H, J = 6.8 Hz); MS (ES) m/z 417 $(MH)^+$. HRMS (FAB): m/z 417.1710 (417.1709 calcd for $C_{19}H_{24}N_6O_3S$ + H^+). Anal. ($C_{19}H_{24}N_6O_3S\cdot1.22\ CF_3CO_2H\cdot0.84H_2O$) C, H, N, F, H_2O.

(2*S*)-2-(Acetylamino)-*N*-[4-[(aminoiminomethyl)amino]-1-(2-benzothiazolylcarbonyl)butyl]-4-methylpentanamide (17). Compound **31** (1.95 g, 3.8 mmol) and 1-acetyl-L-leucine (0.67 g, 3.8 mmol) were converted to crude **17** according to methodology described for **12**. The crude material was purified by reverse-phase HPLC with water/MeCN/CF_3CO_2H (90:10:0.2 to 70:40:0.2) over 60 min to give **17** (217 mg) as a white solid with a HPLC purity of 99.9% and an L/D-arginine epimeric ratio of 1.2:1 by HPLC; ^{1}H NMR δ 0.86 (d, 2.7H), 0.95 (d, 3.3H,), 1.45−1.95 (ov m, 6H), 1.99 (s, 3H), 2.120−2.30 (br m, 1H), 3.21−3.35 (m, 2H), 4.35−4.49 (m, 1H), 5.50−5.6 (m, 0.4H), 5.65−5.73 (m, 0.6H), 7.55−7.70 (m, 2H), 8.13 (d, 1H, J = 7.5 Hz), 8.21 (d, 1H, 6.8 Hz); MS (ES) m/z 447 $(MH)^+$. Anal. ($C_{21}H_{30}N_6O_3S\cdot1.19CF_3CO_2H\cdot0.5H_2O$) C, H, N, F, H_2O.

2-(Acetylamino)-*N*-[4-[(aminoiminomethyl)amino]-1-(2-benzothiazolylcarbonyl)butyl]acetamide (18). Compound **31** (0.501 g, 0.99 mmol) and *N*-acetylglycine (0.175 g, 1.49 mmol) were converted to crude **18** according to methodology described for **12**. The crude material was purified by reverse-phase HPLC with water/MeCN/CF_3CO_2H (90:10:0.2 to 70:40:0.2) over 60 min to give **18** (27 mg) as a white solid with a HPLC purity of 98.0%; ^{1}H NMR δ 1.70−1.95 (m, 3H), 2.01 (s, 3H), 2.10−2.28 (m, 1H), 3.21−3.35 (m, 2H), 3.78, 4.04 (AB_q, 2H, J = 16.6 Hz), 5.70−5.85 (m, 1H), 7.60−7.70 (m, 2H), 8.14 (d, 1H, J = 7.7 Hz), 8.22 (d, 1H, J = 6.8 Hz); MS (ES) m/z 391 (MH^+). HRMS (FAB) m/z = 391.1557 (391.1552 calcd for $C_{17}H_{22}N_6O_3S$ + H^+). Anal. ($C_{17}H_{22}N_6O_3S\cdot1.28CF_3CO_2H\cdot0.3H_2O$) C, H, N, F, H_2O.

(2*S*)-*N*-[4-[(Aminoiminomethyl)amino]-1-(2-benzothiazolylcarbonyl)butyl]-1-(methyl-sulfonyl)-2-pyrrolidinecarboxamide (19). A solution of L-proline *tert*-butyl ester (2.11 g, 12.3 mmol) and triethylamine (3.4 mL, 24.4 mmol) in CH_2Cl_2 (20 mL) was cooled to 5 °C under an argon atmosphere and treated dropwise with methanesulfonyl chloride (0.953 mL, 12.3 mmol). The reaction mixture was filtered through filter agent and extracted sequentially with 10% aqueous citric acid, saturated aqueous $NaHCO_3$, and brine. The organic extract was dried over anhydrous $MgSO_4$ and concentrated in vacuo to give 1-(methylsulfonyl)-L-proline *tert*-butyl ester (2.67 g, 87%). This material was dissolved in 20 mL of trifluoroacetic acid/CH_2Cl_2 (1:1) and stirred at 23 °C for 30 min. The mixture was concentrated in vacuo, triturated with hexane, and placed under 2 Torr of vacuum to give 1-(methylsulfonyl)-L-proline (0.40 g, 22%).

Compound **31** (1.38 g, 2.7 mmol) and 1-(methylsulfonyl)-L-proline (0.40 g, 2.6 mmol) were converted to crude **19** according to methodology described for **12**. The crude material was purified by reverse-phase HPLC with water/MeCN/CF_3CO_2H (90:10:0.2 to 70:40:0.2) over 60 min to give **19** (70 mg) as a white solid with 95.0% purity and an L/D-arginine epimeric ratio of 2.1:1 by HPLC; ^{1}H NMR δ 1.75−2.13 (m, 6H), 2.14−2.35 (m, 2H), 2.95 (s, 2H), 2.99 (s, 1H), 3.22−3.33 (m, 2H), 3.35−3.49 (m, 1H), 3.50−3.61 (m, 1H), 4.23−4.36 (m, 1H), 5.59−5.67 (m, 1H), 7.55−7.70 (m, 2H), 8.12 (d, 1H, J = 7.5 Hz), 8.20−8.29(m, 1H); MS (ES) m/z 467 (MH^+). HRMS (FAB) m/z 467.1533 (467.1535 calcd for $C_{19}H_{26}N_6O_4S_2$ + H^+). Anal. ($C_{19}H_{26}N_6O_4S_2\cdot1.25CF_3CO_2H\cdot1.15H_2O$) C, H, N, F, H_2O.

(2S)-*N*-[(1*S*)-4-[(Aminoiminomethyl)amino]-1-(2-benzothiazolylcarbonyl)butyl]-1-benzoyl-2-pyrrolidinecarboxamide (20). Compound **20** was prepared from L-proline *tert*-butyl ester and benzoyl chloride in a manner analogous to that described for **19**. The crude material was purified by reverse-phase HPLC with water/MeCN/CF_3CO_2H (90:10:0.2 to 60:40:0.2) over 60 min to give **20** (118 mg) as a white solid with 98.3% purity by HPLC and an L/D-arginine epimeric ratio of 2.8:1 by ^{1}H NMR; ^{1}H NMR δ 1.60−2.50 (br m, 6H), 2.17−2.40 (m, 2H) 3.18−3.31 (m, 2H), 3.40−3.65 (m, 2H), 4.55−4.65 (m, 1H), 5.46−5.57 (m, 0.26H), 5.57−5.70 (m, 0.74 H), 7.37−7.7 (ov m, 7H), 8.05−8.25 (m, 2H); MS (ES) m/z 493 (MH^+). Anal. ($C_{25}H_{28}N_6O_3S\cdot1.30CF_3CO_2H\cdot0.75H_2O$) C, H, N, F, H_2O.

(2*S*,4*R*)-1-Acetyl-*N*-[4-[(aminoiminomethyl)amino]-1-(2-thiazolylcarbonyl)butyl]-4-hydroxy-2-pyrrolidinecarboxamide (21). Compound **21** was prepared from *trans*-1-acetyl-4-benzyloxy-L-proline by methods analogous to those described for **6** except that thiazole was used instead of benzothiazole. The crude material was purified by reverse-phase HPLC eluting with a gradient of water/acetonitrile/trifluoroacetic acid (90:10:0.2 to 60:40:0.2) over 60 min to give **21** as a white solid (25 mg) with a HPLC purity of 95.0% and an L/D-arginine epimeric ratio of 2.5:1 by ^{1}H NMR; ^{1}H NMR δ 1.65−1.88 (br m, 3H), 1.95−2.05 (m, 1H), 2.09 (s, 3H), 2.10−2.30 (m, 3.20−3.30, 2H), 3.53 (d, 1H, J = 11.8 Hz), 3.75 (dd, 1H, J = 3.3, 11.8 Hz), 4.4−4.50 (m, 1H), 4.50−4.60 (m, 1H), 5.45−5.60 (br m, 0.29H), 5.60−5.70 (br m, 0.71H), 8.00−8.06 (m, 1H), 8.07−8.20 (m, 1H); MS (ES) m/z 397 (MH^+). HRMS (FAB) m/z 397.1663 (397.1658 calcd for $C_{16}H_{24}N_6O_4S$ + H^+).

(2*S*,4*R*)-1-Acetyl-*N*-[5-amino-1-(2-benzothiazolylcarbonyl)pentyl]-4-hydroxy-2-pyrrolidinecarboxamide (22). A solution of *N*,2-[(1,1-dimethylethoxy)carbonyl]-L-lysine methyl ester hydrochloride (*N*-α-Boc-LysOMe; 5.0 g, 0.0168 mol) in CH_2Cl_2 (80 mL) was treated with 4-methoxy-2,3,6-trimethylbenzenesulfonyl chloride (4.19 g, 0.0168 mol) at 0 °C while stirring under an argon atmosphere. The reaction mixture was allowed to slowly warm to 23 °C over 18 h. The reaction mixture was extracted twice with aqueous 1 M $KHSO_4$, twice with saturated aqueous $NaHCO_3$, and once with brine, dried over anhydrous $MgSO_4$, filtered, and concentrated in vacuo to give *N*-α-Boc-Lys(Mtr)OMe (7.9 g; 99%). This material was dissolved in methanol (150 mL) and treated with 50 mL of 2 M KOH with stirring at 23 °C. After 30 min, the mixture was concentrated in vacuo, and the residue was dissolved in water, acidified to pH 3 with concentrated HCl, and extracted three times with ethyl acetate. The combined extracts were washed twice with brine, dried (Na_2SO_4), and concentrated to yield **32** (Boc-Lys(Mtr)OH (7.7 g, 100%) as a yellow foam.

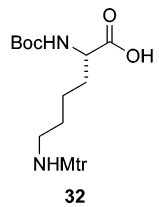

32

Compound **32** (0.92 g, 2.0 mmol) was converted to **22** by methods analogous to those described for **12**, except that the final deprotection was performed in 9:1:1 trifluoroacetic acid/anisole/dimethyl sulfide in the presence of 0.3 M methane-

sulfonic acid over 1 h at 23 °C. The crude material was purified by reverse-phase HPLC with water/MeCN/CF_3CO_2H (90:10:0.2 to 60:40:0.2) over 60 min to give **22** as a white solid (106 mg) with 95.0% purity and an L/D-lysine epimeric ratio of 1.1:1 by HPLC; ^{1}H NMR δ 1.50−1.92 (m, 6H), 1.93−2.07 (m, 1H), 2.10 (s, 3H), 2.11−2.30 (m, 1H), 2.90−3.10 (m, 2H), 3.48−3.58 (m, 1H), 3.70−3.80 (m, 1H), 4.30−4.68 (ov m, 2H), 5.55−5.67 (m, 0.5H), 5.71−5.80 (m, 0.5H), 7.55−7.70 (m, 2H), 8.08 (d, 1H, J = 7.4 Hz), 8.18 (d, 1H, J = 6.8 Hz); MS (ES) m/z 419 (MH^+). Anal. ($C_{20}H_{26}N_4O_4S\cdot0.95CF_3CO_2H\cdot0.05\ CH_3SO_3H\cdot1.55H_2O$) C, H, N, F, S, H_2O.

(2*S*)-1-Acetyl-*N*-[1-(2-benzothiazolylhydroxymethyl)-4-[[imino[amino]methyl]amino]butyl]-2-pyrrolidinecarboxamide (23). Compound **23** was prepared from **31** (2.48 g, 4.9 mmol)) by methods analogous to those described for **12** except that the Dess−Martin oxidation was not performed. The crude material was purified by reverse-phase HPLC (water/MeCN/CF_3CO_2H, 90:10:0.2 to 60:40:0.2) over 60 min to give **22** as a white solid (106 mg) with a HPLC purity of 99%; ^{1}H NMR δ 1.50−2.20 (ov m, 11H), 3.03−3.25 (m, 2H), 3.35−3.57 (m, 2H), 4.23−4.40 (m, 1H), 4.45−4.80 (ov m, 1H), 5.50−5.80 (ov m, 1H), 7.32−7.55 (m, 2H), 7.85−8.01 (m, 2H); MS (ES) m/z 433 (MH^+). HRMS (FAB) m/z 433.2012 (433.2024 calcd for $C_{20}H_{28}N_6O_3S + H^+$).

(2*S*,4*R*)-1-Acetyl-*N*-[1-(2-benzothiazolylcarbonyl)pentyl]-4-hydroxy-2-pyrrolidinecarboxamide (24). Compound **24** was prepared from *N*-*tert*-butoxycarbonyl-L-norvaline (Boc-Nva-OH; 2.5 g, 10.5 mmol) by methods analogous to those described for **6**. The crude material was purified by reverse-phase HPLC with water/MeCN/CF_3CO_2H (90:10:0.2 to 60:40:0.2) over 60 min to give **24** as a white solid (106 mg) with a HPLC purity of 95%. ^{1}H NMR δ 0.90−1.10 (m, 4H), 1.37−1.70 (m, 3H), 1.70−1.90 (m, 1H), 2.05 (s, 3H), 2.10−2.30 (m, 1H), 3.45−3.55 (m, 1H), 3.60−3.80 (m, 1H), 4.30−4.49 (m, 1H), 4.50−4.80 (m, 1H), 5.55−5.75 (m, 1H), 7.55−5.7 (m, 2H), 8.10 (d, 1H, J = 7.4 Hz), 8.20 (d, 1H, J = 6.8 Hz); MS (ES) m/z 390 (MH^+). HRMS (FAB) m/z 390.1480 (390.1488 calcd for $C_{19}H_{23}N_3O_4S + H^+$).

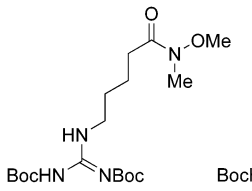

33

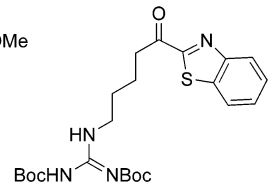

34

1-(2-Benzothiazolyl)-5-[(aminoiminomethyl)amino]-1-pentanone (25). A solution of 5-aminopentanoic acid (0.220 g, 1.88 mmol) and Na_2CO_3 (0.238 g, 2.24 mmol) in 3 mL of water was added dropwise to a solution of 1*H*-pyrazole-1-*N*,*N*′-bis(*tert*-butoxycarbonyl)carboxamidine (0.584 g, 1.88 mmol) in 10 mL of methanol at 23 °C. After 2 h, the reaction mixture was concentrated in vacuo, diluted with water, and extracted twice with ethyl acetate. The aqueous layer was acidified to pH 3 with 1 M $KHSO_4$ and extracted twice with 25 mL of ethyl acetate. The combined extracts were washed with brine, dried ($MgSO_4$), and concentrated. The residue was crystallized from ethyl acetate/hexanes to give 5-[bis(*tert*-butoxycarbonyl)guanidino]pentanoic acid (0.49 g, 72%). This material was combined with *N*,*O*-dimethylhydroxylamine hydrochloride (0.146 g, 1.5 mmol) and triethylamine (0.63 mL, 4.5 mmol), dissolved in DMF (10 mL), and treated with BOP reagent (0.654 g, 1.48 mmol) while stirring under argon at 0 °C. After 30 min, the reaction was quenched with water (1 mL), diluted with ethyl acetate (50 mL), and washed sequentially with water (3×), 10% aqueous citric acid, saturated aqueous $NaHCO_3$, and brine. The organic layer was dried ($MgSO_4$) and concentrated in vacuo. The oily residue was purified by chromatography on silica gel (hexane/EtOAc, 1.5:1) to give **33** (340 mg, 62%).

Butyllithium in hexanes (2.5 M) (2.7 mL, 6.7 mmol) was added dropwise to a stirred solution of distilled benzothiazole (1.1 g, 8.4 mmol) in anhydrous tetrahydrofuran (25 mL) at 78 °C under argon at a rate that kept the reaction temperature below −64 °C. Upon completion of addition, the reaction mixture was stirred for 30 min at −70 °C, and a solution of **33** (0.34 g, 0.84 mmol) in dry tetrahydrofuran (25 mL) was added at a rate that maintained the reaction temperature below −70 °C. The resulting mixture was allowed to slowly warm to 23 °C over 2 h and then quenched with saturated aqueous NH_4Cl (13 mL). The organic layer was separated, washed with brine, dried (Na_2SO_4), and concentrated in vacuo. The residue was triturated three times with hexane and purified by chromatography on silica gel eluting with gradient of 9:1 to 4:1 ethyl acetate/hexane over 30 min to furnish ketone **34** as an amber solid.

Compound **34** (0.14 g, 0.29 mmol) was dissolved in 6 mL of trifluoroacetic acid/CH_2Cl_2 (1:1) and stirred at 23 °C. After 2 h, the reaction mixture was concentrated in vacuo, and the residue was purified by reverse-phase HPLC with water/MeCN/CF_3CO_2H (90:10:0.2) to furnish **25** as a white solid with a HPLC purity of 99%. ^{1}H NMR δ 1.60−1.75 (m, 2H), 1.76−1.95 (m, 2H), 3.14−3.25 (m, 4H), 7.55−5.7 (m, 2H), 8.10 (d, 1H, J = 7.4 Hz), 8.20 (d, 1H, J = 6.8 Hz); MS (ES) m/z 277 (MH^+). HRMS (FAB) m/z 277.1126 (277.1123 calcd for $C_{13}H_{16}N_4OS + H^+$).

***β*-Tryptase Enzyme Assay.** The β-tryptase assay was conducted with human lung β-tryptase (Cortex Biochem #CP3033) in an aqueous buffer (10 mM Tris, 10 mM Hepes, 150 mM NaCl, 0.1% PEG 8000, pH 7.4) using the chromogenic substrate H-D-HHT-Ala-Arg-pNa (American Diagnostica #238)/K_m 580 μM) and a microplate reader (Molecular Devices). IC_{50} experiments were conducted by fixing the enzyme and substrate concentrations (5 nM [E]/715 μM [S]) and varying the inhibitor concentration. Changes in absorbance at 405 nm were monitored using the software program Softmax (Molecular Devices), upon addition of enzyme, with and without inhibitor at 37 °C for 30 min. Percent inhibition was calculated by comparing the initial reaction slopes of samples without inhibitor to those with inhibitor. IC_{50} determination was made using a four-parameter fit logistics model. Inhibition constants (K_i values) were determined under conditions for the analysis of Michaelis−Menten kinetics (1 nM [E]/30−700 μM [S]). Changes in absorbance at 405 nm were monitored (37 °C for 30 min) on addition of enzyme with and without inhibitor present using the software program Softmax (Molecular Devices). Initial reaction slopes of samples were analyzed using the program K-Cat (BioMetallics).

Other Enzyme Assays. Enzyme-catalyzed hydrolysis rates and IC_{50} and K_i values were determined, as described above for β-tryptase, for the following enzymes: trypsin, kallikrein, urokinase plasminogen activator (uPa), plasmin, and thrombin. The enzyme sources, substrates/K_m, aqueous buffer, IC_{50} assay concentrations [E]/[S], and K_i assay concentrations [E]/[S] were as follows: for bovine trypsin (Sigma #T8003), Cbo-Gly-D-Ala-Arg-pNa (American Diagnostica # 216)/K_m 770 μM, buffer A (10 mM Tris, 10 mM Hepes, 150 mM NaCl, 0.1% PEG 8000, pH 7.4), 13.7 nM [E]/1000 μM [S], 13.7 nM [E]/100−3000 μM [S]; for human plasma kallikrein (Sigma #K1004), H-D-Pro-HHT-Arg-pNa (American Diagnostica # 302)/K_m 100 μM, buffer A, 0.025 IU/mL [E]/1000 μM [S], 0.025 IU/mL [E]/30−1000 μM [S]; for human urine uPa (American Diagnostica #124), Cbo-L-(γ)Glu(α-t-BuO)-Gly-Arg-pNa (American Diagnostica #244)/K_m 110 μM, buffer A, 150 U/mL [E]/1000 μM [S], 150 IU/mL [E]/30−1000 μM [S]; for human plasmin (American Diagnostica #421), H-D-Nle-HHT-Lys-pNa (American Diagnostica #251)/K_m 42 μM, buffer A, 1.4 μg/mL [E]/200 μM [S], 1.4 μg/mL [E]/20−500 μM [S]; for human α-thrombin (American Diagnostica #470HT), H-D-HHT-Ala-Arg-pNa (American Diagnostica #238)/K_m 24 μM, buffer A, 0.9 nM [E]/50 μM [S], 0.9 nM [E]/5−100 μM [S].

X-ray Crystallography of the Sulfate Salt of (2*S*)-6.[22] The X-ray crystal structure of (2*S*)-**6**·H_2SO_4 was determined by Crystalytics Company (Lincoln, NE). Single yellowish-orange crystals of (2*S*)-**6**·H_2SO_4 were obtained as thin plates from H_2O/2-propanol (dimensions: 0.09 mm × 0.33 mm × 0.46 mm) and are, at −80 ± 2 °C, monoclinic, space group $P2_1$ −

C_2^2 (No. 4) with $a = 10.653$ (1) Å, $b = 10.425$ (1) Å, $c = 11.448$ (1) Å, $\beta = 108.897$ (2)°, $V = 1202.8$ (2) Å^3 and $Z = 2$ {$d_{calcd} = 1.504$ g cm^{-3}; μ_a (Mo K$_\alpha$) = 0.281 mm^{-1}}. A full hemisphere of diffracted intensities (ω-scan width of 0.30°) was measured by using graphite-monochromated Mo Kα radiation (from a normal-focus sealed X-ray tube operated at 50 kV and 40 mA) on a Bruker Single-Crystal SMART CCD Area Detector Diffraction System. Lattice constants were determined with the Bruker SAINT software package using peak centers for 3134 reflections. A total of 7805 integrated reflection intensities having 2θ(Mo Kα) < 57.47° were produced using the Bruker program SAINT. Of these, 5101 reflections were unique and gave $R_{int} = 0.036$. The Bruker SHELXTL-PC software package was used to solve the structure using "direct methods" techniques. All stages of weighted full-matrix lest-squares refinement were conducted using F_o^2 data with the SHELTX-PC software package. Final agreement factors at convergence are: R_1 (unweighted, based on F) = 0.051 for 3661 independent reflections have 2θ(Mo K$_\alpha$) < 57.47° and $I > 2\sigma(I)$; R_1 (unweighted, based on F) = 0.082 and wR_2 (weighted, based on F^2) = 0.120 for all 5101 independent reflections having 2θ-(Mo K$_\alpha$) < 57.47°.

The structural model incorporated anisotropic thermal parameters for all nonhydrogen atoms and isotropic thermal parameters for all hydrogen atoms. Hydrogen atoms bonded to oxygen and nitrogen were located from a difference Fourier synthesis and included in the structural model as independent isotropic atoms. The methyl group was refined as a rigid rotor (using idealized sp^3-hybridized geometry and a C−H bond length of 0.96 Å) with three rotational parameters in least-squares cycles. The final refined values of these three rotational parameters gave C−C−H angles that ranged from 103° to 119°. The remaining hydrogen atoms were included in the structural model as fixed atoms (using idealized sp^2- or sp^3-hybridized geometry and C−H bond lengths of 0.95−1.00 Å) "riding" on their respective carbons. The isotropic thermal parameters for hydrogen atoms were fixed at values 1.2 (nonmethyl) or 1.5 (methyl) times the equivalent isotropic thermal parameters of the carbon atoms to which they are covalently bonded.

X-ray Crystallography of the (2*S*)-6·Trypsin Complex. Bovine pancreatic trypsin (Worthington Biochemical) was dissolved in 50 mM ammonium acetate buffer (pH 5.6) containing 0.1 w/v% of $CaCl_2$. A solution of (2*S*)-**6** in DMSO was added in a 1.5-fold molar excess. Crystals of (2*S*)-**6**·trypsin were grown at 23 °C by using the hanging-drop, vapor-diffusion technique (drops of 2 mL of protein solution mixed with 2 mL of reservoir solution were equilibrated against a reservoir solution of 0.1 M Tris HCl buffer at pH 7.75 containing 1.2 M $MgSO_4$).[10] The crystals belong to the trigonal space group $P3_121$, with the unit cell parameters: $a = b = 54.67$ Å, $c = 107.87$ Å; $\alpha = \beta = 90°$, $\gamma = 120°$. Diffraction data were collected at −170 °C using 25% glycerol as a cryoprotectant on an R-AXIS IV imaging plate ($R_{merge} = 0.08$; $I/\sigma = 11.5$) and processed with DENZO to a resolution of 1.9 Å.[19a] The completeness of the data at this resolution is 98.6%.

The structure is isomorphous with a previously reported bovine β-trypsin structure (PDB entry 3PTN).[19c] This model, stripped of solvent molecules and calcium ion and with uniform thermal and occupancy parameters, was used for the initial refinement using XPLOR.[19d] Rigid body minimization, followed by simulated annealing with slow cooling,[19e] and conjugate gradient positional refinement were carried out. The molecular model of the inhibitor (2*S*)-**6** was constructed and built into electron density by using CHEMNOTE of the QUANTA program suite. The ideal parameters for the inhibitor were derived from small-molecule structure information from the Cambridge Crystal Data Base.[19f] Manual corrections of the model complex were done during the refinement with the QUANTA graphics program. The refinement data were gradually extended to 1.9 Å resolution during the refinement. Solvent molecules were inserted at reasonable positions where the difference electron density exceeded 2.5 σ. Finally, the individual atomic B-values were refined. The final refinement, performed with the CNS software suite (version 1.0),[19b] converged at $R = 0.175$ and $R_{free} = 0.206$ with 225 water molecules.

Acknowledgment. We thank Rekha Shah and Kristina Klescz for HPLC assay development, Diane Gauthier for NMR analyses, and Fan Zhang-Pasket for the preparation of (2*R*)-**6** and (2*S*)-**6**.

Supporting Information Available: K_i values associated with Table 2 and X-ray crystallographic data for the sulfate salt of (2*S*)-**6**. This material is available free of charge via the Internet at http://pubs.acs.org.

References

(1) (a) Caughey, G. H. *Mast Cell Proteases in Immunology and Biology*; Marcel Dekker: New York, 1995. (b) Caughey, G. H. Of mites and men: trypsin-like proteases in the lungs. *Am. J. Respir. Cell Mol. Biol.* **1997**, *16*, 621−628. (c) Schwartz, L. B. Mast cell tryptase: properties and roles in human allergic responses. *Clin. Allergy Immunol.* **1995**, *6*, 9−23.

(2) (a) Schwartz, L. B. Tryptase: a mast cell serine protease. *Methods Enzymol.* **1994**, *244*, 88−100. (b) Schwartz, L. B.; Lewis, R. A.; Austen, K. F. Tryptase from human pulmonary mast cells. Purification and characterization. *J. Biol. Chem.* **1981**, *256*, 11939−11943.

(3) Pereira, P. J. B.; Bergner, A.; Macedo-Ribeiro, S.; Huber, R.; Matschiner, G.; Fritz, H.; Sommerhoff, C. P.; Bode, W. Human β-tryptase is a ring-like tetramer with active sites facing a central pore. *Nature (London)* **1998**, *392*, 306−311.

(4) (a) Molinari, J. F.; Scuri, M.; Moore, W. R.; Clark, J.; Tanaka, R.; Abraham, W. M. Inhaled tryptase causes bronchoconstriction in sheep via histamine release. *Am. J. Respir. Crit. Care Med.* **1996**, *154*, 649−653. (b) Clark, J.; Abraham, W. M.; Fishman, C. E.; Forteza, R.; Ahmed, A.; Cortes, A.; Warne, R. L.; Moore, W. R.; Tanaka, R. D. Tryptase inhibitors block allergen-induced airway and inflammatory responses in allergic sheep. *Am. J. Respir. Crit. Care Med.* **1995**, *152*, 2076−2083.

(5) (a) Clark, J. M.; Moore, W. R.; Tanaka, R. D. Tryptase inhibitors: a new class of antiinflammatory drugs. *Drugs Future* **1996**, *21*, 811−816. (Update: Anon. APC-366. *Drugs Future* **1998**, *23*, 903.) (b) Rice, K. D.; Tanaka, R. D.; Katz, B. A.; Numerof, R. P.; Moore, W. R. Inhibitors of tryptase for the treatment of mast cell-mediated diseases. *Curr. Pharm. Design* **1998**, *4*, 381−396. (c) Burgess, L. E. Mast cell tryptase as a target for drug design. *Drug News Perspect.* **2000**, *13*, 147−156.

(6) (a) Caughey, G. H.; Raymond, W. W.; Bacci, E.; Lombardy, R. J.; Tidwell, R. R. Bis(5-amidino-2-benzimidazolyl)methane and related amidines are potent, reversible inhibitors of mast cell tryptases. *J. Pharm. Exp. Ther.* **1993**, *264*, 676−682. (b) Burgess, L. E.; Newhouse, B. J.; Ibrahim, P.; Rizzi, J.; Kashem, M. A.; Hartman, A.; Brandhuber, B. J.; Wright, C. D.; Thomson, D. S.; Vigers, G. P. A.; Koch, K. Potent selective nonpeptidic inhibitors of human lung tryptase. *Proc. Natl. Acad. Sci. U.S.A.* **1999**, *96*, 8348−8352. (c) Tidwell, R. R.; Geratz, J. D.; Dubovi, E. J. Aromatic amidines: comparison of their ability to block respiratory syncytial virus induced cell fusion and to inhibit plasmin, urokinase, thrombin and trypsin. *J. Med. Chem.* **1983**, *26*, 294−298.

(7) (a) Molino, M.; Barnathan, E. S.; Numerof, R.; Clark, J.; Dreyer, M.; Cumashi, A.; Hoxie, J. A.; Schechter, N.; Woolkalis, M.; Brass, L. F. Interactions of mast cell tryptase with thrombin receptors and PAR-2. *J. Biol. Chem.* **1997**, *272*, 4043−4049. (b) For reviews on PAR-2, see: Coelho, A.-M.; Ossovskaya, V.; Bunnett, N. W. Proteinase-activated receptor-2: physiological and pathophysiological roles. *Curr. Med. Chem.-Cardiovasc. Hematolog. Agents* **2003**, *1*, 61−72. Scarborough, R. M. Protease-activated receptor-2 antagonists and agonists. *Ibid.* **2003**, *1*, 73−82.

(8) (a) Costanzo, M. J.; Maryanoff, B. E.; Hecker, L. R.; Schott, M. R.; Yabut, S. C.; Zhang, H.-C.; Andrade-Gordon, P.; Kauffman, J. A.; Lewis, J. M.; Krishnan, R.; Tulinsky, A. Potent thrombin inhibitors that probe the S_1' subsite. Tripeptide transition state analogues based on a heterocycle-activated carbonyl group. *J. Med. Chem.* **1996**, *39*, 3039−3043. (b) Giardino, E. C.; Costanzo, M. J.; Kauffman, J. A.; Li, Q. S.; Maryanoff, B. E.; Andrade-Gordon, P. Antithrombotic properties of RWJ-50353, a potent and novel thrombin inhibitor. *Thrombosis Res.* **2000**, *98*, 83−93. (c) Greco, M. N.; Powell, E. T.; Hecker, L. R.; Andrade-Gordon, P.; Kauffman, J. A.; Lewis, J. M.; Ganesh, V.; Tulinsky, A.; Maryanoff, B. E. Novel thrombin inhibitors that are based on a macrocyclic tripeptide motif. *Bioorg. Med. Chem. Lett.* **1996**, *6*, 2947−2952. (d) Maryanoff, B. E.; Greco, M. N.; Zhang, H.-C.; Andrade-Gordon, P.; Kauffman, J. A.; Nicolaou, K. C.; Liu, A.;

Brungs, P. H. Macrocyclic peptide inhibitors of serine proteases. Convergent total synthesis of cyclotheonamides A and B via a late-stage primary amine intermediate. Study of thrombin inhibition under diverse conditions. *J. Am. Chem. Soc.* **1995**, *117*, 1225−1239.

(9) Maryanoff, B. E.; Santulli, R.; McComsey, D. F.; Hoekstra, W. J.; Hoey, K.; Smith, C. E.; Addo, M. F.; Darrow, A. L.; Andrade-Gordon, P. Protease-activated receptor-2 (PAR-2): structure−function study of receptor activation by diverse peptides related to tethered-ligand epitopes. *Arch. Biochem. Biophys.* **2001**, *386*, 195−204.

(10) Recacha, R.; Carson, M.; Costanzo, M. J.; Maryanoff, B.; DeLucas, L. J.; Chattopadhyay, D. Crystal structure of the RWJ-51084·bovine pancreatic *β*-trypsin complex at 1.8 Å. *Acta Crystallogr.* **1999**, *D55*, 1785−1791.

(11) (a) Edwards, P. D.; Meyer, E. F., Jr.; Vijayalakshmi, J.; Tuthill, P. A.; Andisik, D. A.; Gomes, B.; Strimpler, A. J. Design, synthesis, and kinetic evaluation of a unique class of elastase inhibitors, the peptidyl α-ketobenzoxazoles, and the X-ray crystal structure of the covalent complex between porcine pancreatic elastase and Ac−Ala-Pro-Val-2-benzoxazole. *J. Am. Chem. Soc.* **1992**, *114*, 1854−1863. (b) Tsutsumi, S.; Okonogi, T.; Shibahara, S.; Ohuchi, S.; Hatsushiba, E.; Patchett, A. A.; Christansen, B. G. Synthesis and structure−activity relationships of peptidyl α-keto heterocycles as novel inhibitors of prolyl endopeptidase. *J. Med. Chem.* **1994**, *37*, 3492−3502. (c) Matthews, J. H.; Krishnan, R.; Costanzo, M. J.; Maryanoff, B. E.; Tulinsky, A. Crystal structures of thrombin with thiazole-containing inhibitors: probes of the S1′ binding site. *Biophys. J.* **1996**, *71*, 2830−2839.

(12) (a) Costanzo, M. J.; Maryanoff, B. E.; Yabut, S. C. Preparation of peptidyl heterocyclic ketones useful as tryptase inhibitors. PCT patent application WO 0044733 [U.S Patent 6,469,036 (2002)]. (b) In this paper, we use the descriptors *S* and *R* with specific compounds to reflect the absolute stereochemistry at the stereocenter adjacent to the keto group, i.e., at the 2-position, according to the numbering shown for structures **5** and (2*S*)-**6**. The arginine-derived segment of (2*S*)-**6** and its congeners possesses the L-Arg configuration.

(13) The synthesis of **8** without experimental details is reported in the following reference: Klein, S. I.; Dener, J. M.; Molino, B. F.; Gardner, C. J.; D'Alisa, R.; Dunwiddie, C. T.; Kasiewski, C.; Leadley, R. J. *O*-Benzyl hydroxyproline as a bioisostere for Phe-Pro: novel dipeptide thrombin inhibitors. *Bioorg. Med. Chem. Lett.* **1996**, *6*, 2225−2230.

(14) (a) Tosyl-protected Weinreb amide **9** was used for the synthesis of hydroxylated derivatives (e.g., **6**), whereas the corresponding 4-methoxy-2,3,6-trimethylsulfonyl (Mtr)-protected Weinreb amide was preferred for preparing nonhydroxylated derivatives (e.g., **12**). Mtr-protected guanidine intermediates were deprotected with trifluoroacetic acid over 6 h at 23 °C rather than anhydrous HF. (b) We prepared **9** according to the following reference except that crude **9** was triturated with ethyl acetate rather than being crystallized from ethanol: DiMaio, J.; Gibbs, B.; Lefebvre, J.; Konishi, Y.; Munn, D.; Yue, S. Y.; Hornberger, W. Synthesis of a homologous series of ketomethylene arginyl pseudodipeptides and application to low molecular weight hirudin-like thrombin inhibitors. *J. Med. Chem.* **1992**, *35*, 3331−3341. (c) For an alternative preparation of **9**, see: Leung, D.; Schroder, K.; White, H.; Fang, N.-X.; Stoermer, M. J.; Abbenante, G.; Martin, J. L.; Young, P. R.; Fairlie, D. P. Activity of recombinant dengue 2 virus NS3 protease in the presence of a truncated NS2B cofactor, small peptide substrates, and inhibitors. *J. Biol. Chem.* **2001**, *276*, 45762−45771. Also, see: Guichard, G.; Briand, J. P.; Friede, M. Synthesis of arginine aldehydes for the preparation of pseudopeptides. *Peptide Res.* **1993**, *6*, 121−124. (d) For the synthesis of Boc-L-Arg(Mtr)N(OMe)Me, see: Deng, J.; Hamada, Y.; Shioiri, T.; Matsunaga, S.; Fusetani, N. Synthesis of cyclotheonamide B and derivatives. *Angew. Chem. Int. Ed.* **1994**, *33*, 1729−1731. Also, see: Kahn, M. PCT Int. Appl. WO9630396 A1, 1996 (Example 2).

(15) Workup of this reaction was performed with sodium bicarbonate, which is sufficiently alkaline to epimerize the intermediate ketone with prolonged contact. Thus, the desired epimer needs to be isolated and acidified (which stabilizes it against stereomutation) as quickly as possible.

(16) The active diastereomer of **6** possesses the 2*S* configuration (see section on enzyme inhibition). This 2*S* structure is contained in the cocrystal with trypsin (see section on X-ray crystallography) and was confirmed by a separate single-crystal X-ray analysis of the sulfate salt of (2*S*)-**6**, details of which will be published separately.

(17) Katz, B. A.; Clark, J. M.; Finer-Moore, J. S.; Jenkins, T. E.; Johnson, C. R.; Ross, M. J.; Luong, C.; Moore, W. R.; Stroud, R. M. Design of potent selective zinc-mediated protease inhibitors. *Nature (London)* **1998**, *391*, 608−612.

(18) Details of the X-ray crystal structure for (2*S*)-**6**·trypsin will be published separately. Crystallographic coordinates have been deposited with the PDB (RCSB-017762).

(19) (a) Otwinowski, Z.; Minor, W. Processing of X-ray diffraction data collected in oscillation mode. *Methods Enzymol.* **1997**, *276*, 307−326. (b) Brunger, A. T.; Adams, P. D.; Clore, G. M.; DeLano, W. L.; Gros, P.; Grosse-Kunstleve, R, W,; Jiang, J. S.; Kuszewski, J.; Nilges, M.; Pannu, N. S.; Read, R. J.; Rice, L. M.; Simonson, T.; Warren, G. L. Crystallography & NMR System: A new software suite for macromolecular structure determination. *Acta Crystallogr.* **1998**, *D54*, 905−921. (c) Walter, J.; Steigemann, W.; Singh, T. P.; Bartunik, H.; Bode, W.; Huber, R. On the disordered activation domain in trypsinogen: Chemical labeling and low-temperature crystallography. *Acta Crystallogr.* **1982**, *B38*, 1462−1472. (d) Brunger, A. T.; Kuriyan, J.; Karplus, M. Crystallographic R factor refinement by molecular dynamics. *Science* **1987**, *235*, 458−460. (e) Brunger, A. T. Extension of molecular replacement: A new search strategy based on Patterson correlation refinement. *Acta Crystallogr.* **1990**, *A46*, 46−57. (f) Allen, F. H.; Bellard, S.; Brice, M. D.; Cartwright, B. A.; Doubleday: A.; Higgs, H.; Hummelink, T.; Hummelink-Peters, B. G.; Kennard, O.; Motherwell, W. D. S.; Rodgers, J. R.; Watson, D. G. The Cambridge Crystallographic Data Centre: Computer-based search, retrieval, analysis and display of information. *Acta Crystallogr.* **1979**, *B35*, 2331−2339.

(20) The sheep used in this study have a natural airway hypersensitivity to *Ascaris suum* antigen and respond to inhaled antigen with early and late airway responses, as well as subsequent airway hyper-responsiveness. For details on this sheep asthma model, see: Abraham, W. M. Pharmacology of allergen-induced early and late airway responses and antigen-induced airway hyper-responsiveness in allergic sheep. *Pulmonary Pharmacol.* **1989**, *2*, 33−40 (also, see ref 4).

(21) For information relative to the increased electron-withdrawing nature of benzothiazole relative to thiazole, see: (a) Chan, A. W. E.; Golec, J. M. C. Prediction of relative potency of ketone protease inhibitors using molecular orbital theory. *Bioorg. Med. Chem.* **1996**, *4*, 1673−1677. (b) Edwards, P. D.; Wolanin, D. J.; Andisik, D. W.; Davis, M. W. Peptidyl α-ketoheterocyclic inhibitors of human neutrophil elastase. 2. Effect of varying the heterocyclic ring on in vitro potency. *J. Med. Chem.* **1995**, *38*, 76−85. (c) Reference 8a.

(22) See the paragraph at the end of this paper regarding Supporting Information.

JM030050P